Research Article

Khadijeh Sadri*, Kamyar Hosseini, Soheil Salahshour, Dumitru Baleanu, Ali Ahmadian, and Choonkil Park*

Efficient scheme for a category of variable-order optimal control problems based on the sixth-kind Chebyshev polynomials

https://doi.org/10.1515/dema-2024-0034
received September 12, 2022; accepted May 24, 2024

Abstract: The main goal of the present study is to introduce an operational collocation scheme based on sixth-kind Chebyshev polynomials (SCPs) to solve a category of optimal control problems involving a variable-order dynamical system (VODS). To achieve this goal, the collocation method based on SCPs, the pseudo-operational matrix for the fractional integral operator, and the dual operational matrix are adopted. More precisely, an algebraic equation is obtained instead of the objective function and a system of algebraic equation is derived instead of the VODS. The constrained equations obtained from joining the objective function to the VODS are ultimately optimized using the method of the Lagrange multipliers. Detailed convergence analysis of the suggested method is given as well. Four illustrative examples along with several tables and figures are formally provided to support the efficiency and preciseness of the numerical scheme.

Keywords: variable-order optimal control problems, operational collocation method, sixth-kind Chebyshev polynomials, convergence analysis

MSC 2020: 34H05, 34A08, 33C45

1 Introduction

Fractional operators exhibit real-world phenomena better due to their memory properties unlike their classic counterparts. Diverse definitions have been presented for integral and derivative operators with fractional orders that the most applicable are the Caputo and Riemann-Liouville operators [1–6]. The variable-order integration and derivative are extensions of their classical definitions. In fractional integral and derivative operators with variable orders, the orders depend on the time variable or the space variable or both of them that nowadays have much popularity in various fields of engineering and science [7–15]. In addition, Kashif

*** Corresponding author: Khadijeh Sadri,** Mathematics Research Center, Near East University TRNC, Mersin 10, Nicosia 99138, Turkey; Department of Mathematics, Near East University TRNC, Mersin 10, Nicosia 99138, Turkey; Faculty of Art and Science, University of Kyrenia, Kyrenia, TRNC, Mersin 10, Turkey, e-mail: kh.sadri@uma.ac.ir, khadijeh.sadrikhatouni@neu.edu.tr
*** Corresponding author: Choonkil Park,** Research Institute for Natural Sciences, Hanyang University, Seoul 04763, South Korea, e-mail: baak@hanyang.ac.kr
Kamyar Hosseini: Department of Mathematics, Near East University TRNC, Mersin 10, Nicosia 99138, Turkey; Department of Computer Science and Mathematics, Lebanese American University, Beirut, Lebanon
Soheil Salahshour: Faculty of Engineering and Natural Sciences, Istanbul Okan University, Istanbul, Turkey; Faculty of Engineering and Natural Sciences, Bahcesehir University, Istanbul, Turkey; Faculty of Science and Letters, Piri Reis University, Tuzla, Istanbul, Turkey
Dumitru Baleanu: Department of Computer Science and Mathematics, Lebanese American University, Beirut, Lebanon; Institute of Space Sciences, Magurele-Bucharest, R 76900, Romania
Ali Ahmadian: Faculty of Engineering and Natural Sciences, Istanbul Okan University, Istanbul, Turkey; Decisions Lab, Mediterranea University of Reggio Calabria, Reggio Calabria, Italy

et al. applied an efficient variable-order Bernstein collocation technique to a nonlinear coupled system of variable-order reaction-diffusion equations [16]. Ganji and Jafari considered the shifted Legendre and shifted Chebyshev polynomials for solving multi-variable orders differential equations [17]. Jafari et al. [18] proposed a numerical approach based on the shifted fifth-kind Chebyshev polynomials to study a category of variable-order integro-differential equations. Precise modeling of fractional functional equations emerged in diverse problems of engineering, such as the bioengineering, viscoelasticity, and dynamics of interfaces between substrates and nanoparticles, gives rise to variable-order optimal control problems (VOCPs) via joining these equations to an objective function and a set of initial and/or boundary conditions [19–22]. Tajadodi [8] used Genocchi polynomials to solve a type of VOCP. Dehestani et al. [19] used fractional-order Bessel wavelets for numerically solving these equations. Heydari et al. [20] applied the Chebyshev cardinal functions to VFOCPs with dynamical systems of weakly singular variable-order integral equations. Hassani and Avazzadeh [22] used the transcendental Bernstein series for solving nonlinear VFOCPs. Heydari [23], Heydari and Avazzadeh [24] introduced new direct methods based on the Chebyshev cardinal functions and the wavelet method for VFOCPs. A Legendre collocation method and a nonstandard finite difference method were proposed to solve VFOCPs in [25,26].

The spectral methods along with orthogonal polynomials as basis functions are very popular and efficient. The Galerkin, Tau, and collocation are the three most widely used methods of the family of the spectral methods. The Chebyshev polynomials of the first to fourth kinds have many applications as basis functions in the spectral methods [27–33]. The other two sorts of Chebyshev polynomials are called the Chebyshev polynomials of the fifth and sixth kinds that have been applied to solve some fractional ordinary differential equations [34–36]. After introducing the Chebyshev polynomials of the sixth kind by Masjed-Jamei [37] and due to the complex structure of this category of polynomials and their weight functions compared to the first- and second-kind Chebyshev polynomials, researchers and mathematicians have rarely used it as a basis in spectral methods. Although recently, Chebyshev polynomials of the sixth type have been considered as basis functions in spectral methods for solving fractional Rayleigh-Stokes problems, time-fractional heat equations, and hyperbolic-telegraph problems [38–41]. This work shows efficiency of these polynomials by obtaining a suitable approximate solution to the problem under study. The aim of the current work is to achieve the following:

- Establishing an operational collocation scheme based on the sixth-kind shifted Chebyshev polynomials for solving the variable-order Caputo control problems with boundary conditions.
- Displaying the accuracy of the suggested method via estimating an error bound for the residual function in a Chebyshev-weighted Sobolev space.
- Acquiring more precise approximations to the problems under study compared to approximations reported in previous studies [19,42].
- Considering the best approximation to the exact solution in a Chebyshev-weighted space for finding the error bound in addition to considering the approximate solution obtained from the suggested method.

Hence, in the present work, a numerical scheme is constructed by coupling the collocation method and the sixth-kind Chebyshev polynomials (SCPs) as the basis functions for solving the following VOCP:

$$\text{Min } \mathcal{J}[\mathrm{x}, \mathrm{u}] = \int_0^1 \mathcal{F}(t, \mathrm{x}(t), \mathrm{u}(t))\mathrm{d}t, \tag{1.1}$$

$${}_0^C\mathcal{D}_t^{\theta(t)}\mathrm{x}(t) = \mathcal{G}(t, \mathrm{x}(t), \dot{\mathrm{x}}(t), \mathrm{u}(t)), \quad 0 < \theta(t) \leqslant 1, \tag{1.2}$$

with the conditions

$$\mathrm{x}(0) = \eta_0, \quad \mathrm{x}(1) = \eta_1, \tag{1.3}$$

where $\mathrm{x}(t)$ and $\mathrm{u}(t)$ are the state and control variables, respectively, η_0 and η_1 are the real constants, $\mathcal{F}$ and $\mathcal{G}$ are the smooth functions, ${}_0^C\mathcal{D}_t^{\theta(t)}$ is the variable-order derivative operator in the Caputo sense, and $t \in J = [0, 1]$

is the time variable. $\mathrm{x}(t)$, $\mathrm{u}(t)$, and their derivatives are continuous functions and there exist finite constants $\mathcal{M}_{i,\mathrm{x}}$ for $i = 1, 2$, $\mathcal{M}_{1,\mathrm{u}}$, and $\mathcal{M}_{\theta}$ such that

$$|\mathrm{x}(t)| \leq \mathcal{M}_{1,\mathrm{x}}, \quad |\dot{\mathrm{x}}(t)| \leq \mathcal{M}_{1,\dot{\mathrm{x}}}, \quad |\mathrm{u}(t)| \leq \mathcal{M}_{1,\mathrm{u}}, \quad |{}_0^C\mathcal{D}_t^{\theta(t)}\mathrm{x}(t)| \leq \mathcal{M}_{\theta}.$$

In this respect, first a pseudo-operational matrix for the fractional integration and a dual operational matrix (related to the product of basis vectors) for the SCPs are derived. The stated and control variables are approximated by the operational matrices and the basis vector. Approximations are substituted into performance index (1.1), variable-order dynamical system (VODS) (1.2), and conditions (1.3). These approximations and matrices avoid the direct use of the integration and derivative operations. Thus, the given problem is converted into a set of algebraic equations. In the next step, constraint equations obtained from the algebraic system are joined to the performance index using a set of unknown Lagrange multipliers. Ultimately, optimal conditions provide a nonlinear system of algebraic equations, by solving which, unknown coefficients are determined.

This study is structured as follows: some definitions of variable-order operators are given in Section 2. The Chebyshev polynomials of the sixth kind, some of their properties, and their operational matrices are presented in Section 3. In Section 4, the suggested approach is explained. Error bounds for approximate solutions and the residual functions of the performance index and VODS are calculated in Section 5. The efficiency and accuracy of the proposed approach are illustrated by reporting numerical results in Section 6. Section 7 concludes briefly.

2 Preliminary definitions

Definition 2.1. The variable-order derivative in the Caputo sense of the order $\theta(t)(\theta : [0,1] \to (0,1])$ of the differentiable function f is defined as [19]:

$${}_0^C\mathcal{D}_t^{\theta(t)}\mathsf{f}(t) = \begin{cases} \mathsf{f}'(t), & \theta(t) = 1, \\ \dfrac{1}{\Gamma(1-\theta(t))}\displaystyle\int_0^t (t-s)^{-\theta(t)}\mathsf{f}'(s)\mathrm{d}s, & \text{otherwise}. \end{cases} \tag{2.1}$$

The following results are obtained based on the above definition:

$$\begin{aligned} &(1)\quad {}_0^C\mathcal{D}_t^{\theta(t)}A = 0, && A \text{ is a constant}, \\ &(2)\quad {}_0^C\mathcal{D}_t^{\theta(t)}{}_0^C\mathcal{D}_t^{\vartheta(t)}\mathsf{f}(t) = {}_0^C\mathcal{D}_t^{\theta(t)+\vartheta(t)}\mathsf{f}(t), \\ &(3)\quad {}_0^C\mathcal{D}_t^{\theta(t)}t^{\nu} = \begin{cases} \dfrac{\Gamma(\nu+1)t^{\nu-\theta(t)}}{\Gamma(\nu-\theta(t)+1)}, & \nu \geqslant 1, \\ 0, & \text{otherwise}. \end{cases} \end{aligned}$$

Definition 2.2. The variable-order integral in the Riemann-Liouville sense with the order $\theta(t)$ of the continuous function f is as follows [20]:

$${}_0^{RL}\mathcal{I}_t^{\theta(t)}\mathsf{f}(t) = \begin{cases} \dfrac{1}{\Gamma(\theta(t))}\displaystyle\int_0^t (t-s)^{\theta(t)-1}\mathsf{f}(s)\mathrm{d}s, & \theta(t) > 0, \\ \mathsf{f}(t), & \theta(t) = 0. \end{cases} \tag{2.2}$$

Based on Definition (2.2), the following properties are obtained:

$$\begin{aligned} &(1)\quad {}_0^C\mathcal{D}_t^{\theta(t)}\mathsf{f}(t) = {}_0^{RL}\mathcal{I}_t^{1-\theta(t)}\mathsf{f}'(t), \\ &(2)\quad {}_0^{RL}\mathcal{I}_t^{\theta(t)}t^{\nu} = \frac{\Gamma(\nu+1)t^{\nu+\theta(t)}}{\Gamma(\nu+\theta(t)+1)}. \end{aligned}$$

3 SCPs and their operational matrices

In this section, the SCPs are introduced and their operational matrices are constructed.

3.1 SCPs

These polynomials are defined over the interval $[-1, 1]$ as follows [36,43]:

$$\bar{\mathcal{Y}}_j(t) = \bar{\mathcal{S}}_j^{-5,2,-1,1}(t), \quad t \in [-1, 1],$$

where

$$\bar{\mathcal{S}}_j^{-5,2,-1,1}(t) = \left(\prod_{l=0}^{\left\lfloor \frac{j}{2} \right\rfloor} \frac{(2l + (-1)^{j+1} + 2) + 2}{-\left(2l + (-1)^{j+1} + 2\left\lfloor \frac{j}{2} \right\rfloor\right) - 5} \right) \mathcal{S}_j^{-5,2,-1,1}(t), \quad j \geqslant 0,$$

$$\mathcal{S}_j^{-5,2,-1,1}(t) = \sum_{r=0}^{\left\lfloor \frac{j}{2} \right\rfloor} \binom{\left\lfloor \frac{j}{2} \right\rfloor}{r} \left(\prod_{l=0}^{\left\lfloor \frac{j}{2} \right\rfloor - r - 1} \frac{-\left(2l + (-1)^{j+1} + 2\left\lfloor \frac{j}{2} \right\rfloor\right) - 5}{(2l + (-1)^{j+2} + 2) + 2} \right) t^{j-2r}, \quad j \geqslant 0.$$

These polynomials satisfy the following recurrence formula:

$$\bar{\mathcal{Y}}_j(t) = t\bar{\mathcal{Y}}_{j-1}(t) - \frac{j(j+1) + (-1)^j(2j+1) + 1}{4j(j+1)} \bar{\mathcal{Y}}_{j-2}(t), \quad j \geqslant 2, \ t \in [-1, 1],$$
$$\bar{\mathcal{Y}}_0(t) = 1, \quad \bar{\mathcal{Y}}_1(t) = t.$$

The SCPs are orthogonal with respect to the weight function $\bar{w}(t) = t^2\sqrt{1 - t^2}$, i.e.,

$$\int_{-1}^{1} \bar{\mathcal{Y}}_i(t)\bar{\mathcal{Y}}_j(t)\bar{w}(t)\mathrm{d}t = \bar{h}_i\delta_{ij},$$

where δ_{ij} is the Kronecker delta function and

$$\bar{h}_i = \begin{cases} \dfrac{\pi}{2^{2i+3}}, & i \,\text{even}, \\ \dfrac{\pi(i+3)}{2^{2i+3}(i+1)}, & i \,\text{odd}. \end{cases}$$

By means of the change in variable $t \leftarrow 2t - 1$, the shifted sixth-kind Chebyshev polynomials (SSKCPs) are orthogonal regarding the weight function $w(t) = (2t - 1)^2\sqrt{t - t^2}$ on $J = [0, 1]$, i.e.,

$$\int_{0}^{1} \mathcal{Y}_i(t)\mathcal{Y}_j(t)w(t)\mathrm{d}t = \hbar_i\delta_{ij},$$

where

$$\hbar_i = \begin{cases} \dfrac{\pi}{2^{2i+5}}, & i \ \text{even}, \\ \dfrac{\pi(i+3)}{2^{2i+5}(i+1)}, & i \ \text{odd}. \end{cases} \tag{3.1}$$

Abd-Elhameed and Youssri [36] presented a series form of the SSKCPs as follows:

$$\mathcal{Y}_j(t) = \sum_{r=0}^{j} \varsigma_{r,j} t^r, \tag{3.2}$$

where

$$\varsigma_{r,j} = \frac{2^{2r-j}}{(2r+1)!} \begin{cases} \sum_{l=\left\lfloor \frac{r+1}{2} \right\rfloor}^{\frac{j}{2}} \frac{(-1)^{\frac{j}{2}+l+r}(2l+r+1)!}{(2l-r+1)!}, & j \text{ even}, \\ \frac{2}{j+1} \sum_{l=\left\lfloor \frac{r}{2} \right\rfloor}^{\frac{j-1}{2}} \frac{(-1)^{\frac{j+1}{2}+l+r}(l+1)(2l+r+2)!}{(2l-r+1)!}, & j \text{ odd}. \end{cases} \tag{3.3}$$

Please refer to [40,41] for more properties and details about SCPs.

A square-integrable function $z(t) \in L_w^2(J)$ can be written in terms of the SSKCPs as

$$z(t) = \sum_{j=0}^{\infty} Z_j \mathcal{Y}_j(t), \quad t \in J, \tag{3.4}$$

where the coefficients Z_j are calculated as

$$Z_j = \frac{1}{\hbar_j} \int_0^1 z(t) \mathcal{Y}_j(t) w(t) \mathrm{d}t, \quad j = 0, 1, 2, \ldots.$$

The first few terms in (3.4) are practically used to determine an approximation to $z(t)$, i.e.,

$$z(t) \approx z_N(t) = \sum_{j=0}^{N} Z_j \mathcal{Y}_j(t) = \mathbf{Y}^T(t)\mathbf{Z} = \mathbf{Z}^T\mathbf{Y}(t), \tag{3.5}$$

where $\mathbf{Y}(t)$ and $\mathbf{Z}$ are the $(N+1)$-order vectors as follows:

$$\mathbf{Y}(t) = [\mathcal{Y}_0(t)\mathcal{Y}_1(t) \ldots \mathcal{Y}_N(t)]^T, \quad \mathbf{Z} = [Z_0 Z_1 \ldots Z_N]^T. \tag{3.6}$$

3.2 Operational matrices for SSKCPs

To solve the problem (1.1)–(1.3), three types of operational matrices are needed: an integral operational matrix of integer order, a pseudo-operational integral matrix of fractional order, and a dual operational matrix. In order to construct them, some lemmas and theorems must be given.

Lemma 3.1. *If $\rho > -1$, one has*

$$\int_0^1 t^\rho \mathcal{Y}_k(t) w(t) \mathrm{d}t = \sum_{m=0}^{k} \varsigma_{m,k} \frac{\sqrt{\pi}}{2} \left\{ \frac{4\Gamma(\rho+m+\frac{7}{2})}{\Gamma(\rho+m+5)} - \frac{4\Gamma(\rho+m+\frac{5}{2})}{\Gamma(\rho+m+4)} + \frac{\Gamma(\rho+m+\frac{3}{2})}{\Gamma(\rho+m+3)} \right\}.$$

Proof. See Lemma 4.2 in [43]. □

Theorem 3.2. *If $\mathbf{Y}(t)$ is the basis vector in* (3.6)*, then the integral of the vector $\mathbf{Y}(t)$ can be attained as*

$$\int_0^t \mathbf{Y}(s)\mathrm{d}s \approx \mathbf{P}\mathbf{Y}(t), \quad t \in J,$$

where $\mathbf{P}$ *is the* $(N+1)\times(N+1)$ *integral operational matrix corresponding to the basis vector with integer powers as follows*:

$$\mathbf{P} = \begin{bmatrix} p_0^0 & p_1^0 & \dots & p_N^0 \\ p_0^1 & p_1^1 & \dots & p_N^1 \\ \vdots & \vdots & \ddots & \vdots \\ p_0^N & p_1^N & \dots & p_N^N \end{bmatrix}, \tag{3.7}$$

and its entries are computed as

$$p_k^j = \sum_{\mathfrak{r}=0}^{j} \frac{\varsigma_{\mathfrak{r},j}\sqrt{\pi}}{2(\mathfrak{r}+1)\hbar_k} \sum_{\mathfrak{m}=0}^{k} \varsigma_{\mathfrak{m},k} \left(\frac{4\Gamma(\mathfrak{r}+\mathfrak{m}+\frac{9}{2})}{\Gamma(\mathfrak{r}+\mathfrak{m}+6)} - \frac{4\Gamma(\mathfrak{r}+\mathfrak{m}+\frac{7}{2})}{\Gamma(\mathfrak{r}+\mathfrak{m}+5)} + \frac{\Gamma(\mathfrak{r}+\mathfrak{m}+\frac{5}{2})}{\Gamma(\mathfrak{r}+\mathfrak{m}+4)} \right), \quad j = 0,1,\dots,N, \ \ k = 0,1,\dots,N.$$

Proof. See Theorem 4.3 in [43]. □

Theorem 3.3. *Suppose that* $\mathbf{Y}(t)$ *is the basis vector in* (3.6) *and* ${}_0^{RL}\mathcal{I}_t^{\theta(t)}$, $\theta(t) \in (0,1]$, *is the Riemann-Liouville fractional integral of the order* $\theta(t)$. *Then, one has*

$${}_0^{RL}\mathcal{I}_t^{\theta(t)}\mathbf{Y}(t) \approx \mathbf{P}^{(\theta)}\mathbf{Y}(t),$$

where $\mathbf{P}^{(\theta)}$ *is the* $(N+1)\times(N+1)$ *fractional operational matrix as follows*:

$$\mathbf{P}^{(\theta)} = \begin{bmatrix} p^{(\theta)}(0,0) & p^{(\theta)}(0,1) & \dots & p^{(\theta)}(0,N) \\ p^{(\theta)}(1,0) & p^{(\theta)}(1,1) & \dots & p^{(\theta)}(1,N) \\ \vdots & \vdots & \ddots & \vdots \\ p^{(\theta)}(N,0) & p^{(\theta)}(N,1) & \dots & p^{(\theta)}(N,N) \end{bmatrix},$$

where $p^{(\theta)}(i,k)$ *are calculated as*

$$p^{(\theta)}(i,k) = \sum_{\mathfrak{r}=0}^{i} \frac{\varsigma_{\mathfrak{r},i}\sqrt{\pi}\Gamma(\mathfrak{r}+1)t^{\theta(t)}}{2\Gamma(\mathfrak{r}+\theta(t)+1)\hbar_k} \sum_{\mathfrak{m}=0}^{k} \varsigma_{\mathfrak{m},k} \left(\frac{4\Gamma(\mathfrak{r}+\mathfrak{m}+\frac{7}{2})}{\Gamma(\mathfrak{r}+\mathfrak{m}+5)} - \frac{4\Gamma(\mathfrak{r}+\mathfrak{m}+\frac{5}{2})}{\Gamma(\mathfrak{r}+\mathfrak{m}+4)} + \frac{\Gamma(\mathfrak{r}+\mathfrak{m}+\frac{3}{2})}{\Gamma(\mathfrak{r}+\mathfrak{m}+3)} \right),$$

$i = 0, 1, \dots, N, \ \ k = 0, 1, \dots, N.$

Proof. See Theorem 4.4 in [43]. □

Lemma 3.4. *Suppose that* $\mathcal{Y}_j(t)$ *and* $\mathcal{Y}_k(t)$ *are the jth and kth SSKCPs, respectively. The product of* $\mathcal{Y}_j(t)$ *and* $\mathcal{Y}_k(t)$ *is written as the series form*

$$Q_{j+k}(t) = \mathcal{Y}_j(t)\mathcal{Y}_k(t) = \sum_{\mathfrak{r}=0}^{j+k} q_{\mathfrak{r}}^{(j,k)} t^{\mathfrak{r}}, \quad j,k = 0,1,\dots,N,$$

where the coefficients $q_{\mathfrak{r}}^{(j,k)}$, $j,k = 0,1,\dots,N$, *are computed as*

If $j \geqslant k$:
$\mathfrak{r} = 0,1,\dots,j+k$,
if $\mathfrak{r} > j$, *then*
$q_{\mathfrak{r}}^{(j,k)} = \sum_{\mathfrak{l}=\mathfrak{r}-j}^{k} \varsigma_{\mathfrak{r}-\mathfrak{l},j}\varsigma_{\mathfrak{l},k}$,
else
$\mathfrak{r}_1 = \min\{\mathfrak{r}, k\}$,
$q_{\mathfrak{r}}^{(j,k)} = \sum_{\mathfrak{l}=0}^{\mathfrak{r}_1} \varsigma_{\mathfrak{r}-\mathfrak{l},j}\varsigma_{\mathfrak{l},k}$,
end.

If $j < k$:
$\mathfrak{r} = 0,1,\dots,j+k$,
if $r \leqslant j$, *then*
$\mathfrak{r}_1 = \min\{\mathfrak{r}, j\}$,

$q_{\mathfrak{r}}^{(j,k)} = \sum_{\mathfrak{l}=0}^{\mathfrak{r}_1} \zeta_{\mathfrak{r}-\mathfrak{l},j}\zeta_{\mathfrak{l},k}$,
else
$\mathfrak{r}_2 = \min\{\mathfrak{r}, k\}$,
$q_{\mathfrak{r}}^{(j,k)} = \sum_{\mathfrak{l}=\mathfrak{r}-j}^{\mathfrak{r}_2} \zeta_{\mathfrak{r}-\mathfrak{l},j}\zeta_{\mathfrak{l},k}$,
end.

Proof. See Lemma 3 in [44]. □

Theorem 3.5. *If* $\mathbf{Y}(t)$ *is the basis vector in* (3.6)*, then the integration of the product of the vectors* $\mathbf{Y}(t)$ *and* $\mathbf{Y}^{\mathbf{T}}(t)$ *over* $[0, 1]$ *is given as the following matrix form*:

$$\int_0^1 \mathbf{Y}(t)\mathbf{Y}^T(t)\mathrm{d}t = \mathbf{D}\mathbf{Y}(t), \tag{3.8}$$

where $\mathbf{D}$ *is the* $(N + 1) \times (N + 1)$ *dual operational matrix and its members are as follows*:

$$d_{j,k} = \sum_{\mathfrak{r}=0}^{j+k} \frac{q_{\mathfrak{r}}^{(j,k)}}{\mathfrak{r} + 1}, \quad j, k = 0, 1, \ldots, N.$$

Proof. From the left-hand side of equation (3.8), one has

$$\int_0^1 \mathbf{Y}(t)\mathbf{Y}^T(t)\mathrm{d}t = \left[\int_0^1 \mathcal{Y}_j(t)\mathcal{Y}_k(t)\mathrm{d}t\right]_{j,k}, \quad j, k = 0, 1, \ldots, N.$$

By utilizing Lemma 3.4, the integration of the product of $\mathcal{Y}_j(t)$ and $\mathcal{Y}_k(t)$ can be computed as

$$\int_0^1 \mathcal{Y}_j(t)\mathcal{Y}_k(t)\mathrm{d}t = \sum_{r=0}^{j+k} q_r^{(j,k)} \int_0^1 t^{\mathfrak{r}}\mathrm{d}t = \sum_{\mathfrak{r}=0}^{j+k} \frac{q_{\mathfrak{r}}^{(j,k)}}{\mathfrak{r} + 1}, \quad j = 0, 1, \ldots, N, k = j = 0, 1, \ldots, N.$$

Thus, the desired result is obtained. □

Interested readers can refer to [45] to understand the matrix algebra done within the work.

4 Methodology

In this section, the derived matrices in Section 3 are employed to numerically solve problems (1.1)–(1.3). For this end, pursuing the following steps is proposed:
Step 1. The control variable is expanded as

$$u(t) \approx \sum_{k=0}^{N} U_k\mathcal{Y}_k(t) = \mathbf{Y}^T(t)\mathbf{U}, \quad \text{s.t. } \mathbf{U} = [U_0U_1 \ldots U_N]^T. \tag{4.1}$$

Step 2-1. If both functions $\dot{\mathrm{x}}(t)$ and ${}_0^C\mathcal{D}_t^{\theta(t)}\mathrm{x}(t)$, $0 < \theta(t) < 1$, exist in the dynamical system, then

$$\dot{\mathrm{x}}(t) \approx \sum_{k=0}^{N} X_k\mathcal{Y}_k(t) = \mathbf{Y}^T(t)\mathbf{X}, \quad \text{s.t. } \mathbf{X} = [X_0X_1 \ldots X_N]^T. \tag{4.2}$$

Now, integrating approximate (4.2) and using Theorem 3.2 lead to an approximation to the state variable:

$$\begin{aligned} \mathrm{x}(t) &\approx \mathbf{Y}^T(t)\mathbf{P}^T\mathbf{X} + \mathrm{x}(0) \approx \mathbf{Y}^T(t)\mathbf{P}^T\mathbf{X} + \mathbf{Y}^T(t)\mathbf{F} \\ &\approx \mathbf{Y}^T(t)\mathbf{V}_1, \quad \text{s.t. } \mathbf{V}_1 = \mathbf{P}^T\mathbf{X} + \mathbf{F}. \end{aligned} \tag{4.3}$$

Step 2-2. An approximation is obtained to ${}_0^C\mathcal{D}_t^{\theta(t)}\mathrm{x}(t)$, $0 < \theta(t) < 1$, by means of approximation (4.2):

$$ {}_0^C\mathcal{D}_t^{\theta(t)}\mathrm{x}(t) = {}_0^{RL}\mathcal{I}_t^{1-\theta(t)}\dot{\mathrm{x}}(t) \approx \mathbf{Y}^T(t)\mathbf{X}. \tag{4.4}$$

By applying the operator ${}_0^{RL}\mathcal{I}_t^{1-\theta(t)}$ on (4.4) and using Theorem 3.3, one obtains the following approximation:

$$ {}_0^C\mathcal{D}_t^{\theta(t)}\mathrm{x}(t) \approx \mathbf{Y}^T(t)\mathbf{P}^{(1-\theta)T}\mathbf{X} = \mathbf{Y}^T(t)\mathbf{V}_2, \quad \text{s.t. } \mathbf{V}_2 = \mathbf{P}^{(1-\theta)T}\mathbf{X}. \tag{4.5}$$

Step 2-3. If the function $\dot{\mathrm{x}}(t)$ does not exist in dynamical system (1.2), then

$$ {}_0^C\mathcal{D}_t^{\theta(t)}\mathrm{x}(t) \approx \mathbf{Y}^T(t)\mathbf{X}. \tag{4.6}$$

Applying the operator ${}_0^{RL}\mathcal{I}_t^{\theta(t)}$ on (4.6) leads to an approximation to the state variable:

$$ \begin{aligned} \mathrm{x}(t) &\approx \mathbf{Y}^T(t)\mathbf{P}^{(\theta)T}\mathbf{X} + \mathrm{x}(0) \\ &= \mathbf{Y}^T(t)\mathbf{P}^{(\theta)T}\mathbf{X} + \mathbf{Y}^T(t)\mathbf{F} \\ &= \mathbf{Y}^T(t)\mathbf{V}_1, \quad \text{s.t. } \mathbf{V}_1 = \mathbf{P}^{(\theta)T}\mathbf{X} + \mathbf{F}. \end{aligned} \tag{4.7}$$

Step 3. Substituting approximations (4.1)–(4.7) into dynamical system (1.2), one obtains

$$ \mathcal{M}(t, \theta(t)) = \mathbf{Y}^T(t)\mathbf{P}^{(1-\theta)T}\mathbf{X} - \mathcal{G}(t, \mathbf{Y}^T(t)\mathbf{V}_1, \mathbf{Y}^T(t)\mathbf{X}, \mathbf{Y}^T(t)\mathbf{U}). \tag{4.8}$$

Step 4. If $t_i, i = 0, 1, \ldots, N$, are roots of $\mathcal{Y}_{N+1}(t)$, then collocating $\mathcal{M}(t, \theta(t))$ in (4.8) leads to the following algebraic system:

$$ \mathcal{M}(t_i, \theta(t_i)) = \mathbf{Y}^T(t_i)\mathbf{P}^{(1-\theta_i)T}\mathbf{X} - \mathcal{G}(t_i, \mathbf{Y}^T(t_i)\mathbf{V}_1, \mathbf{Y}^T(t_i)\mathbf{X}, \mathbf{Y}^T(t_i)\mathbf{U}), \quad i = 0, 1, \ldots, N. \tag{4.9}$$

Step 5. The boundary condition $\mathrm{x}(1) = \eta_1$ can be approximated by (4.3) or (4.7) as follows:

$$ \mathcal{B}_1 = \mathbf{Y}^T(1)\mathbf{V}_1 - \eta_1. \tag{4.10}$$

Step 6. Substituting approximations (4.1), (4.3), or (4.7) into performance index (1.1) leads to the following expression:

$$ \mathcal{J}[\mathrm{x}, \mathrm{u}] \approx \mathcal{J}_N = \int_0^1 \mathcal{F}(t, \mathbf{Y}^T(t)\mathbf{V}_1, \mathbf{Y}^T(t)\mathbf{U})\mathrm{d}t. \tag{4.11}$$

Step 7. The following optimization problem is constructed by means of (4.9), (4.10), and (4.11).

$$ \mathcal{J}_N^* = \mathcal{J}_N + \mathbf{\Lambda}^T\mathbf{M} + \lambda_{N+1}\mathcal{B}_1, \tag{4.12}$$

where $\mathbf{\Lambda}, \mathbf{M}$ are $(N+1)$-order vectors as

$$ \mathbf{\Lambda} = [\lambda_0\lambda_1 \ldots \lambda_N], \quad \mathbf{M}_i = [\mathcal{M}(t_i, \theta(t_i))], \quad i = 0, 1, \ldots, N, $$

and λ_i, $0 \leqslant i \leqslant N+1$, are unknown Lagrange multipliers.

Step 8. The necessary conditions for obtaining the extremum of the problem are

$$ \frac{\partial \mathcal{J}_N^*}{\partial \mathbf{X}} = 0, \quad \frac{\partial \mathcal{J}_N^*}{\partial \mathbf{U}} = 0, \quad \frac{\partial \mathcal{J}_N^*}{\partial \mathbf{\Lambda}} = 0, \quad \frac{\partial \mathcal{J}_N^*}{\partial \lambda_{N+1}} = 0. \tag{4.13}$$

Step 9. Solving algebraic system (4.13) involving $3N + 4$ equations leads to determine the vectors $\mathbf{X}, \mathbf{U}, \mathbf{\Lambda}$, and the coefficient λ_{N+1}. Thus, approximate optimal solutions for the given problem are obtained.

5 Error bounds

In the current section, some upper bounds for errors of approximate solutions and the residual function of the performance index are obtained in a Sobolev space.

Definition 5.1. Suppose that $\mathcal{Y}_j(t)$ is the SSKCP of at most degree N and $\mathbb{P}_N = \text{span}\{\mathcal{Y}_0(t), \mathcal{Y}_1(t), ..., \mathcal{Y}_N(t)\}$. If $v(t) \in C(J)$, then there exists $\bar{v}(t) \in \mathbb{P}_N$ such that

$$\|v(t) - \bar{v}(t)\| = \inf_{y \in \mathbb{P}_N} \|v(t) - y(t)\|,$$

where $\bar{v}(t)$ is the best approximation to $v(t)$ from $\mathbb{P}_N$.

Definition 5.2. The Chebyshev-weighted Sobolev space $C\mathcal{H}_w^{\varpi}(J)$, $\varpi \in \mathbb{Z}^+ \cup \{0\}$ is defined as

$$C\mathcal{H}_w^{\varpi}(J) = \left\{ v(t) \,\middle|\, \frac{\mathrm{d}^k v(t)}{\mathrm{d}t^k} \in L_w^2(J), 0 \leqslant k \leqslant \varpi \right\},$$

where $L_w^2(J)$ is the weighted space of squared-integrable functions on the interval J and equipped to the following norm and semi-norm

$$\|v\|_{C\mathcal{H}_w^{\varpi}(J)} = \left(\sum_{k=0}^{\varpi} \left\| \frac{\mathrm{d}^k v}{\mathrm{d}t^k} \right\|_{L_w^2(J)}^2 \right)^{\frac{1}{2}}, \quad |v|_{C\mathcal{H}_w^{\varpi,N}(J)} = \left(\sum_{k=\min\{\varpi, N+1\}}^{\varpi} \left\| \frac{\mathrm{d}^k v}{\mathrm{d}t^k} \right\|_{L_w^2(J)}^2 \right)^{\frac{1}{2}}, \tag{5.1}$$

where $\|\cdot\|_{L_w^2(J)}$ is the L_w^2-norm defined as

$$\|f\|_{L_w^2(J)} = \left(\int_0^1 |f(t)|^2 w(t) \mathrm{d}t \right)^{\frac{1}{2}}.$$

Theorem 5.1. *Suppose that $v(t) \in C\mathcal{H}_w^{\varpi}(J)$, $\varpi \in \mathbb{Z}^+ \cup \{0\}$, and $\bar{v}_N(t) = \sum_{j=0}^{N} \bar{V}_j \mathcal{Y}_j(t)$ is the best approximation to $v(t)$ from $\mathbb{P}_N$. Then, one obtains* [46]:

$$\|v - \bar{v}_N\|_{L_w^2(J)} \leqslant \beta N^{-\varpi} |v|_{C\mathcal{H}_w^{\varpi,N}(J)} \tag{5.2}$$

and

$$\left\| \frac{\mathrm{d}^m v}{\mathrm{d}t^m} - \frac{\mathrm{d}^m \bar{v}_N}{\mathrm{d}t^m} \right\|_{C\mathcal{H}_w^m(J)} \leqslant \beta N^{\rho(m)-\varpi} |v|_{C\mathcal{H}_w^{m,\varpi,N}(J)}, \quad 0 \leqslant m \leqslant \varpi, \tag{5.3}$$

where

$$\rho(m) = \begin{cases} 2m - \dfrac{1}{2}, & m > 0, \\ 0, & m = 0, \end{cases} \quad |v|_{C\mathcal{H}_w^{m,\varpi,N}(J)} = \left(\sum_{k=\min\{\varpi, N+1\}}^{\varpi} N^{2m-2k} \left\| \frac{\mathrm{d}^k v}{\mathrm{d}t^k} \right\|_{L_w^2(J)}^2 \right)^{\frac{1}{2}}$$

and β depends on ϖ.

Theorem 5.2. *Suppose that $v_N^*(t) = \sum_{j=0}^{N} V_j^* \mathcal{Y}_j(t) = \mathbf{Y}^T(t)\mathbf{V}^*$ and $\bar{v}_N(t) = \sum_{j=0}^{N} \bar{V}_j \mathcal{Y}_j(t) = \mathbf{Y}^T(t)\bar{\mathbf{V}}$ are the approximate solutions obtained from the presented method and the best approximation to $v(t)$ from $\mathbb{P}_N$, respectively. Then, one obtains*

$$\|v - v_N^*\|_{L_w^2(J)} \leqslant \beta N^{-\varpi} |v|_{C\mathcal{H}_w^{\varpi,N}(J)} + \|\bar{\mathbf{V}} - \mathbf{V}^*\|_2 \left(\sum_{j=0}^{N} \hbar_j \right)^{\frac{1}{2}},$$

where $\hbar_j, j = 0, 1, \ldots, N$, are defined in (3.1).

Proof. The following inequality is obtained from the properties of the norm

$$\|v - v_N^*\|_{L_w^2(J)} \leqslant \|v - \bar{v}_N\|_{L_w^2(J)} + \|\bar{v}_N - v_N^*\|_{L_w^2(J)}. \tag{5.4}$$

The second norm in the right-hand side of (5.4) is as follows:

$$\begin{aligned}
\|\bar{v} - v_N^*\|_{L_w^2(J)} &= \|\mathbf{Y}^T(t)\bar{\mathbf{V}} - \mathbf{Y}^T(t)\mathbf{V}^*\|_{L_w^2(J)} = \left\| \sum_{j=0}^{N} \bar{V}_j \mathcal{Y}_j(t) - \sum_{j=0}^{N} V_j^* \mathcal{Y}_j(t) \right\|_{L_w^2(J)} \\
&= \left\| \sum_{j=0}^{N} (\bar{V}_j - V_j^*) \mathcal{Y}_j(t) \right\|_{L_w^2(J)} = \left(\int_0^1 \left| \sum_{j=0}^{N} (\bar{V}_j - V_j^*) \mathcal{Y}_j(t) \right|^2 w(t) \mathrm{d}t \right)^{\frac{1}{2}} \\
&\leqslant \left(\sum_{j=0}^{N} |\bar{V}_j - V_j^*|^2 \right)^{\frac{1}{2}} \left(\int_0^1 \sum_{j=0}^{N} |\mathcal{Y}_j(t)|^2 w(t) \mathrm{d}t \right)^{\frac{1}{2}} \\
&= \|\bar{\mathbf{V}} - \mathbf{V}^*\|_2 \left(\int_0^1 \sum_{j=0}^{N} |\mathcal{Y}_j(t)|^2 w(t) \mathrm{d}t \right)^{\frac{1}{2}} \\
&= \|\bar{\mathbf{V}} - \mathbf{V}^*\|_2 \left(\sum_{j=0}^{N} \hbar_j \right)^{\frac{1}{2}}.
\end{aligned}$$

It can be easily seen from relation (3.1), $\hbar_j$, $0 \leqslant j \leqslant N$, are decreasing when j (or N) is sufficiently large. Using Theorem 5.1 and the recent result, inequality (5.4) is written as

$$\|v - v_N^*\|_{L_w^2(J)} \leqslant \beta N^{-\varpi} |v|_{\mathcal{CH}_w^{\varpi,N}(J)} + \|\bar{\mathbf{V}} - \mathbf{V}^*\|_2 \left(\sum_{j=0}^{N} \hbar_j \right)^{\frac{1}{2}}. \qquad \square$$

Theorem 5.3. *Assume that $v(t) \in \mathcal{CH}_w^m(J)$, $\varpi \in \mathbb{Z}^+ \cup \{0\}$, $v_N^*(t)$ is the approximate solution of the proposed method, $\bar{v}_N(t)$ is the best approximation to $v(t)$ from $\mathbb{P}_N$, ${}_0^C\mathcal{D}_t^{\theta(t)} v_N^*(t) \approx \mathbf{Y}^T(t)\mathbf{W}^*$, ${}_0^C\mathcal{D}_t^{\theta(t)} \bar{v}_N(t) \approx \mathbf{Y}^T(t)\bar{\mathbf{W}}$, and $0 < \theta(t) \leqslant 1$. Then, one obtains*

$$\|{}_0^C\mathcal{D}_t^{\theta(t)} v - {}_0^C\mathcal{D}_t^{\theta(t)} v_N^*\|_{L_w^2(J)} \leqslant \beta\beta_1 N^{\rho(m)-\varpi} |v|_{\mathcal{CH}_w^{\varpi,N}(J)} + \|\bar{\mathbf{W}} - \mathbf{W}^*\|_2 \left(\sum_{j=0}^{N} \hbar_j \right)^{\frac{1}{2}}.$$

Proof. Based on Definition 2.2, one has

$$\begin{aligned}
\|{}_0^C\mathcal{D}_t^{\theta(t)} v - {}_0^C\mathcal{D}_t^{\theta(t)} \bar{v}_N\|_{L_w^2(J)} &= \left\| \frac{1}{\Gamma(1-\theta(t))} \int_0^t (t-s)^{-\theta(t)} v'(s) \mathrm{d}s - \frac{1}{\Gamma(1-\theta(t))} \int_0^t (t-s)^{-\theta(t)} \bar{v}_N'(s) \mathrm{d}s \right\|_{L_w^2(J)} \\
&= \left\| \frac{1}{\Gamma(1-\theta(t))} \int_0^t (t-s)^{-\theta(t)} (v'(s) - \bar{v}_N'(s)) \mathrm{d}s \right\|_{L_w^2(J)}.
\end{aligned} \tag{5.5}$$

Besides, one has for $t_0 \in J$

$$\frac{1}{\Gamma(1-\theta(t))} \int_0^t (t-s)^{-\theta(t)} \mathrm{d}s = \frac{t^{1-\theta(t)}}{\Gamma(2-\theta(t))} \leqslant \frac{t_0^{\theta^*}}{\Gamma(\theta^{**})} = \beta_1,$$

where $\theta^* = \sup_{t\in J}(1-\theta(t))$, $\theta^{**} = \inf_{t\in J}(2-\theta(t))$. Therefore, by setting $m = 1$ in (5.3), equation (5.5) is as follows:

$$\begin{aligned}
\|{}_0^C\mathcal{D}_t^{\theta(t)} v - {}_0^C\mathcal{D}_t^{\theta(t)} \bar{v}_N\|_{L_w^2(J)} &\leqslant \beta_1 \int_0^t \|v'(s) - \bar{v}_N'(s)\|_{L_w^2(J)} \mathrm{d}s \leqslant \beta_1 \|v'(s) - \bar{v}_N'(s)\|_{L_w^2(J)} \\
&\leqslant \beta_1 \|v'(s) - \bar{v}_N'(s)\|_{\mathcal{CH}_w^1(J)} \leqslant \beta_1 \beta N^{\frac{3}{2}-\varpi} |v|_{\mathcal{CH}_w^{1,\varpi,N}(J)}.
\end{aligned}$$

According to the given approximations to ${}_0^C\mathcal{D}_t^{\theta(t)}\bar{v}_N$ and ${}_0^C\mathcal{D}_t^{\theta(t)}v_N^*$ and Theorem 5.2, one has

$$\|{}_0^C\mathcal{D}_t^{\theta(t)}\bar{v}_N - {}_0^C\mathcal{D}_t^{\theta(t)}v_N^*\|_{L_w^2(J)} = \|\mathbf{Y}^T(t)\bar{\mathbf{W}} - \mathbf{Y}^T(t)\mathbf{W}^*\|_{L_w^2(J)} \leqslant \|\bar{\mathbf{W}} - \mathbf{W}^*\|_2 \left(\sum_{j=0}^{N}\hbar_j\right)^{\frac{1}{2}}.$$

Thus, the desired result is achieved and the following relation is deduced:

$$\|{}_0^C\mathcal{D}_t^{\theta(t)}v - {}_0^C\mathcal{D}_t^{\theta(t)}v_N^*\|_{L_w^2(J)} \longrightarrow 0 \quad \text{as } N \longrightarrow \infty. \qquad \square$$

Now, suppose that $\mathrm{x}_N^*(t)$ and $\mathrm{u}_N^*(t)$ are approximate optimal solutions obtained from the present method and the operators $\mathcal{F}$ and $\mathcal{G}$ satisfy the Lipschitz conditions. Therefore, using Theorems 5.2 and 5.3, one obtains

$$\int_0^1 \mathcal{F}(t, \mathrm{x}(t), \mathrm{u}(t))\mathrm{d}t - \int_0^1 \mathcal{F}(t, \mathrm{x}_N^*(t), \mathrm{u}_N^*(t))\mathrm{d}t - \mathcal{H}_N(t) = 0,$$

where $\mathcal{H}_N(t)$ is the residual function. So, taking norm leads to the following inequality:

$$\begin{aligned}\|\mathcal{H}_N\|_{L_w^2(J)} &= \|\mathcal{F}(t, \mathrm{x}, \mathrm{u}) - \mathcal{F}(t, \mathrm{x}_N^*, \mathrm{u}_N^*)\|_{L_w^2(J)} \\ &\leqslant s_1(\|\mathrm{x} - \mathrm{x}_N^*\|_{L_w^2(J)} + \|\mathrm{u} - \mathrm{u}_N^*\|_{L_w^2(J)}) \\ &\leqslant s_1\left(\beta N^{-\varpi}(|\mathrm{x}|_{\mathcal{CH}_w^{\varpi,N}} + |\mathrm{u}|_{\mathcal{CH}_w^{\varpi,N}}) + \sqrt{\sum_{j=0}^{N}\hbar_j}(\|\bar{\mathbf{X}} - \mathbf{X}^*\|_2 + \|\bar{\mathbf{U}} - \mathbf{U}^*\|_2)\right)\end{aligned} \tag{5.6}$$

and

$${}_0^C D_t^{\theta(t)}\mathrm{x}(t) - {}_0^C D_t^{\theta(t)}\mathrm{x}_N^*(t) - \mathcal{G}(t, \mathrm{x}(t), \dot{\mathrm{x}}(t), \mathrm{u}(t)) + \mathcal{G}(t, \mathrm{x}_N^*(t), \dot{\mathrm{x}}_N^*(t), \mathrm{u}_N^*(t)) + \mathcal{R}_N(t) = 0,$$

where $\mathcal{R}_N(t)$ is the residual function. Similarly, the following inequality is achieved:

$$\begin{aligned}\|\mathcal{R}_N\|_{L_w^2(J)} &= \|{}_0^C D_t^{\theta(t)}\mathrm{x} - \mathcal{G}(t, \mathrm{x}, \dot{\mathrm{x}}, \mathrm{u}(t)) - {}_0^C D_t^{\theta(t)}\mathrm{x}_N^* + \mathcal{G}(t, \mathrm{x}_N^*, \dot{\mathrm{x}}_N^*, \mathrm{u}_N^*)\|_{L_w^2(J)} \\ &\leqslant \|{}_0^C D_t^{\theta(t)}\mathrm{x} - {}_0^C D_t^{\theta(t)}\mathrm{x}_N^*\|_{L_w^2(J)} + s_2(\|\mathrm{x} - \mathrm{x}_N^*\|_{L_w^2(J)} + \|\dot{\mathrm{x}} - \dot{\mathrm{x}}_N^*\|_{L_w^2(J)} + \|\mathrm{u} - \mathrm{u}_N^*\|_{L_w^2(J)}) \\ &\leqslant \beta\beta_1 N^{\frac{3}{2}-\varpi}\,|\mathrm{x}|_{\mathcal{CH}_w^{1,\varpi,N}} + \sqrt{\sum_{j=0}^{N}\hbar_j}\,\|\bar{\mathbf{W}} - \mathbf{W}^*\|_2 \\ &\quad + s_2\left(\beta N^{-\varpi}(|\mathrm{x}|_{\mathcal{CH}_w^{\varpi,N}} + |\mathrm{u}|_{\mathcal{CH}_w^{\varpi,N}}) + \sqrt{\sum_{j=0}^{N}\hbar_j}(\|\bar{\mathbf{X}} - \mathbf{X}^*\|_2 + \|\bar{\mathbf{U}} - \mathbf{U}^*\|_2) + \beta N^{\frac{3}{2}-\varpi}\,|\mathrm{x}|_{\mathcal{CH}_w^{1,\varpi,N}}\right).\end{aligned} \tag{5.7}$$

It can be easily seen that when $N \to \infty$, the right-hand sides of inequalities (5.6) and (5.7) tend to zero. It can be seen that when N is large enough $\|\bar{\mathbf{W}} - \mathbf{W}^*\|_2, \|\bar{\mathbf{X}} - \mathbf{X}^*\|_2, \|\bar{\mathbf{U}} - \mathbf{U}^*\|_2 \to 0$. Thus, the error bounds will be proportional to $N^{-\varpi}$. The obtained bounds show an exponential rate of convergence.

6 Numerical experiments

The efficiency and preciseness of the present approach are exemplified by solving four illustrated examples.

Example 6.1. Consider the following fractional-order optimal control problem [47]:

$$\mathrm{Min}\,\mathcal{J}[\mathrm{x}, \mathrm{u}] = \int_0^1 (t\mathrm{u}(t) - (\theta(t) + 2)\mathrm{x}(t))^2\mathrm{d}t,$$

$$\dot{\mathrm{x}}(t) + {}_0^C\mathcal{D}_t^{\theta(t)}\mathrm{x}(t) - \mathrm{u}(t) - t^2 = 0, \quad 0 < \theta(t) \leqslant 1,$$

with the following boundary conditions:

$$\mathrm{x}(0) = 0, \quad \mathrm{x}(1) = \frac{2}{\Gamma(3+\theta(t))}.$$

The exact solutions are $(\mathrm{x}(t), \mathrm{u}(t), \mathcal{J}[\mathrm{x}, \mathrm{u}]) = (\frac{2t^{\theta(t)+2}}{\Gamma(3+\theta(t))}, \frac{2t^{\theta(t)+1}}{\Gamma(2+\theta(t))}, 0)$. To determine the approximate optimal solutions by the scheme described in Section 4, the following approximations can be considered:

$$\begin{gathered}\dot{\mathrm{x}}(t) \approx \mathbf{Y}^T(t)\mathbf{X}, \quad \mathrm{x}(t) \approx \mathbf{Y}^T(t)\mathbf{P}^T\mathbf{X} = \mathbf{Y}^T(t)\mathbf{V}_1, \quad \mathbf{V}_1 = \mathbf{P}^T\mathbf{X}, \\ {}_0^C\mathcal{D}_t^{\theta(t)}\mathrm{x}(t) \approx \mathbf{Y}^T(t)\mathbf{P}^{(1-\theta)^T}\mathbf{X}, \quad \mathrm{u}(t) \approx \mathbf{Y}^T(t)\mathbf{U}.\end{gathered} \tag{6.1}$$

Substituting approximations (6.1) into the performance index, the dynamical system, and the boundary conditions, one obtains

$$\begin{gathered}\mathcal{J}_N = \int_0^1 (t\mathbf{Y}^T(t)\mathbf{U} - (\theta(t)+2)\mathbf{Y}^T(t)\mathbf{P}^T\mathbf{X})^2 \mathrm{d}t, \\ \mathcal{M}(t, \theta(t)) = \mathbf{Y}^T(t)\mathbf{X} + \mathbf{Y}^T(t)\mathbf{P}^{(1-\theta(t))}\mathbf{X} - \mathbf{Y}^T(t)\mathbf{U} - t^2, \\ \mathcal{B}_1 = \mathbf{Y}^T(1)\mathbf{P}^T\mathbf{X} - \frac{2}{\Gamma(3+\theta(t))}.\end{gathered}$$

Finally, the following optimization problem is achieved:

$$\mathcal{J}_N^* = \mathcal{J}_N + \mathbf{\Lambda}^T\mathbf{M} + \lambda_{N+1}\mathcal{B}_1.$$

Based on the procedure stated in Section 4, the unknown vectors and coefficients are determined. The maximum absolute errors related to the approximately optimal solutions are compared to those reported in [19] and [47] in Table 1 for $N = 3$ and $\theta(t) = 1$. The comparison of the results shows the accuracy of the proposed scheme. Also, the computational time is 2.07 s. The absolute errors of the approximate solutions at the points $t_i = 0.2i$, $i = 0, 1, \ldots, 5$, are listed in Table 2 for $N = 3, 5$, and $\theta(t) = 0.9$. The values of the functional $\mathcal{J}[\mathrm{x}, \mathrm{u}]$ are 8.3946×10^{-8} and 1.2254×10^{-10} for $N = 3$ and 5, respectively. The plots of the exact and approximate solutions and absolute error functions are depicted in Figure 1 for $N = 5$ and $\theta(t) = 1$. The numerical results confirm the satisfactory agreement of the approximate results with their exact ones.

Table 1: Maximum absolute errors of state and control variables for $N = 3$ and $\theta(t) = 1$ of Example 6.1

	Present method	**Method in [19]**	**Method in [47]**
Error of $\mathrm{x}(t)$	1.3536×10^{-21}	3.5526×10^{-4}	9.3698×10^{-15}
Error of $\mathrm{u}(t)$	4.3136×10^{-20}	9.1353×10^{-3}	5.6882×10^{-16}
$\mathcal{J}[\mathrm{x}, \mathrm{u}]$	1.3433×10^{-40}	—	0

Table 2: Absolute errors of numerical results at selected points for $N = 3, 5$ and $\theta(t) = 0.9$ of Example 6.1

	$N = 3$			$N = 5$		
t_i	**Error of** $\mathrm{x}(t)$	**Error of** $\mathrm{u}(t)$	$\mathcal{J}[\mathrm{x}(t), \mathrm{u}(t)]$	**Error of** $\mathrm{x}(t)$	**Error of** $\mathrm{u}(t)$	$\mathcal{J}[\mathrm{x}(t), \mathrm{u}(t)]$
0.0	1.8707×10^{-4}	4.3125×10^{-3}	8.3946×10^{-8}	7.09718×10^{-6}	5.6699×10^{-4}	1.2254×10^{-10}
0.2	1.5189×10^{-4}	4.6587×10^{-4}		2.9405×10^{-6}	3.0923×10^{-5}	
0.4	8.8858×10^{-5}	3.9267×10^{-4}		8.0242×10^{-6}	6.7222×10^{-5}	
0.6	5.2670×10^{-5}	1.9803×10^{-4}		7.6123×10^{-6}	2.6087×10^{-5}	
0.8	1.8546×10^{-4}	4.2251×10^{-4}		3.5419×10^{-6}	2.1047×10^{-5}	
1.0	0	5.0222×10^{-4}		1.0000×10^{-20}	2.0350×10^{-5}	

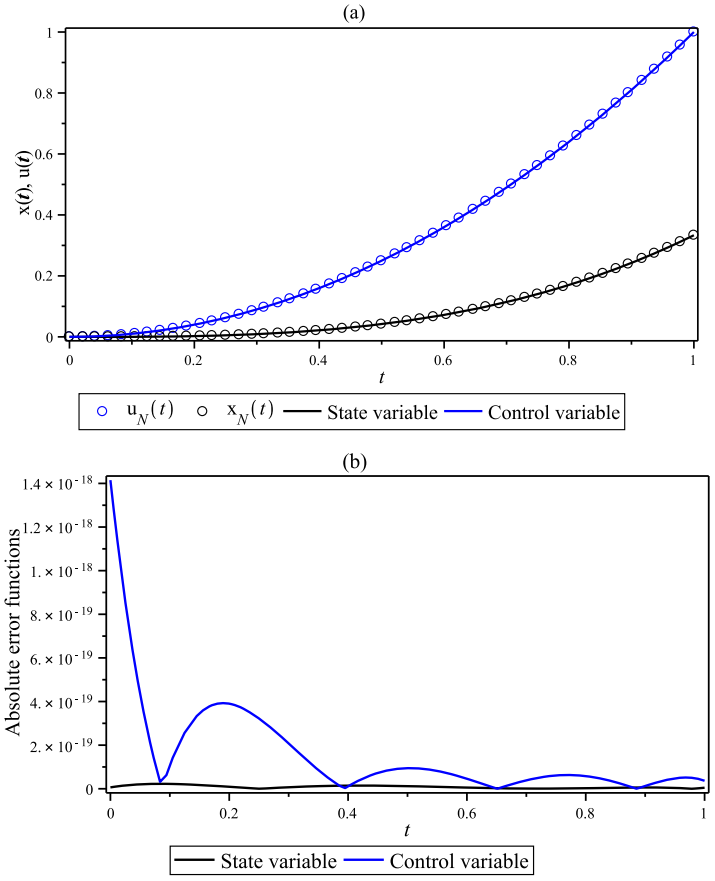

Figure 1: (a) Exact and approximate solutions and (b) absolute error functions of Example 6.1 for $N = 5$ and $\theta(t) = 1$.

Table 3: Absolute errors of approximate optimal solutions for $N = 5$ and different values of $\theta(t)$ of Example 6.2

	$\theta(t) = 0.45$		$\theta(t) = 0.47$		$\theta(t) = 0.49$	
t_i	$x_N(t)$	$u_N(t)$	$x_N(t)$	$u_N(t)$	$x_N(t)$	$u_N(t)$
0	3.1265×10^{-5}	1.1897×10^{-4}	3.0469×10^{-5}	1.1745×10^{-4}	2.9581×10^{-5}	1.1544×10^{-4}
0.2	3.5212×10^{-6}	6.0441×10^{-5}	3.4425×10^{-6}	5.9910×10^{-5}	3.3576×10^{-6}	5.9204×10^{-5}
0.4	4.0384×10^{-5}	1.4253×10^{-4}	3.9372×10^{-5}	1.3977×10^{-4}	3.8250×10^{-5}	1.3658×10^{-4}
0.6	1.9546×10^{-5}	8.8103×10^{-5}	1.9320×10^{-5}	8.6704×10^{-5}	1.9028×10^{-5}	8.5049×10^{-5}
0.8	5.7962×10^{-6}	1.1813×10^{-4}	5.8273×10^{-6}	1.1542×10^{-5}	5.8329×10^{-6}	1.1236×10^{-4}
1	2.0000×10^{-20}	7.9133×10^{-5}	2.0000×10^{-20}	7.7584×10^{-5}	2.0000×10^{-20}	7.5740×10^{-5}
$\mathcal{J}[x_N, u_N]$	8.7213×10^{-9}		8.3862×10^{-9}		8.0067×10^{-9}	

Table 4: Values of functional $\mathcal{J}[x, u]$ for $N = 5$ and $\theta(t) = 0.7, 0.8, 0.9, 1$ of Example 6.2

	$\theta(t) = 0.7$	$\theta(t) = 0.8$	$\theta(t) = 0.9$	$\theta(t) = 1$
Present method	3.0974×10^{-9}	1.2969×10^{-9}	2.8560×10^{-10}	9.1863×10^{-41}
Method in [19]	1.5115×10^{-8}	7.0650×10^{-9}	1.7599×10^{-9}	0
Method in [42]	—	1.649×10^{-8}	4.264×10^{-9}	3.023×10^{-33}

Table 5: Values of functional $\mathcal{J}[x, u]$ for $N = 7$ and different values of $\theta(t)$ of Example 6.2

	$\theta(t) = 0.8 + 0.05\sin(t)$	$\theta(t) = 0.8 + 0.005\sin(t)$	$\theta(t) = 0.8 + 0.0005\sin(t)$	$\theta(t) = 0.8$
Present method	4.3839×10^{-5}	4.6827×10^{-7}	4.7798×10^{-9}	1.2969×10^{-9}
Method in [19]	1.5854×10^{-7}	4.8728×10^{-8}	4.0839×10^{-8}	7.0650×10^{-9}

Table 6: Absolute errors of approximate optimal solutions for $N = 5$ and different values of $\theta(t)$ of Example 6.2

	$\theta(t) = 0.8 + 0.05\sin(t)$		$\theta(t) = 0.8 + 0.005\sin(t)$		$\theta(t) = 0.8 + 0.0005\sin(t)$	
t_i	$x_N(t)$	$u_N(t)$	$x_N(t)$	$u_N(t)$	$x_N(t)$	$u_N(t)$
0	5.9048×10^{-5}	8.5540×10^{-3}	7.4315×10^{-6}	8.9703×10^{-4}	1.4460×10^{-6}	9.1429×10^{-5}
0.2	7.265×10^{-4}	7.8584×10^{-3}	7.3547×10^{-5}	8.0564×10^{-4}	7.2622×10^{-6}	8.1172×10^{-5}
0.4	1.3218×10^{-3}	6.8141×10^{-3}	1.3489×10^{-4}	6.8654×10^{-4}	1.3864×10^{-5}	6.9438×10^{-5}
0.6	1.5487×10^{-3}	8.9384×10^{-3}	1.5707×10^{-4}	9.2494×10^{-4}	1.5120×10^{-5}	9.2738×10^{-5}
0.8	1.1184×10^{-3}	7.0338×10^{-3}	1.1199×10^{-4}	7.2347×10^{-4}	1.0504×10^{-5}	7.2285×10^{-5}
1	2.0000×10^{-20}	5.6181×10^{-3}	2.0000×10^{-20}	6.0555×10^{-4}	0.0000	6.1417×10^{-5}
$\mathcal{J}[x_N, u_N]$	4.3839×10^{-5}		4.6827×10^{-7}		4.7798×10^{-9}	

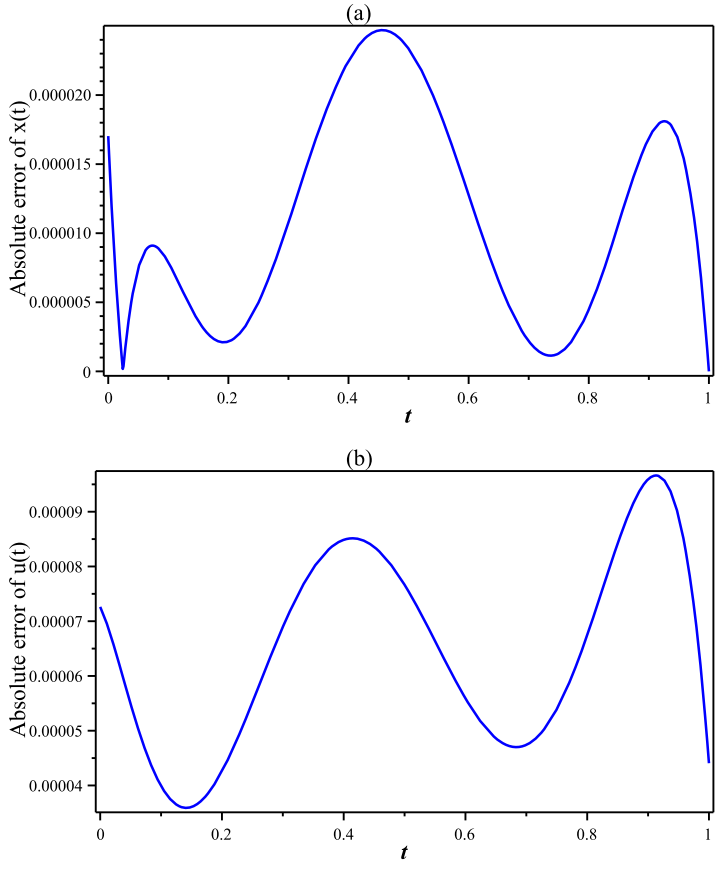

Figure 2: Plots of error functions for (a) $x(t)$, (b) $u(t)$ for $N = 5$ and $\theta(t) = 0.7$ of Example 6.2.

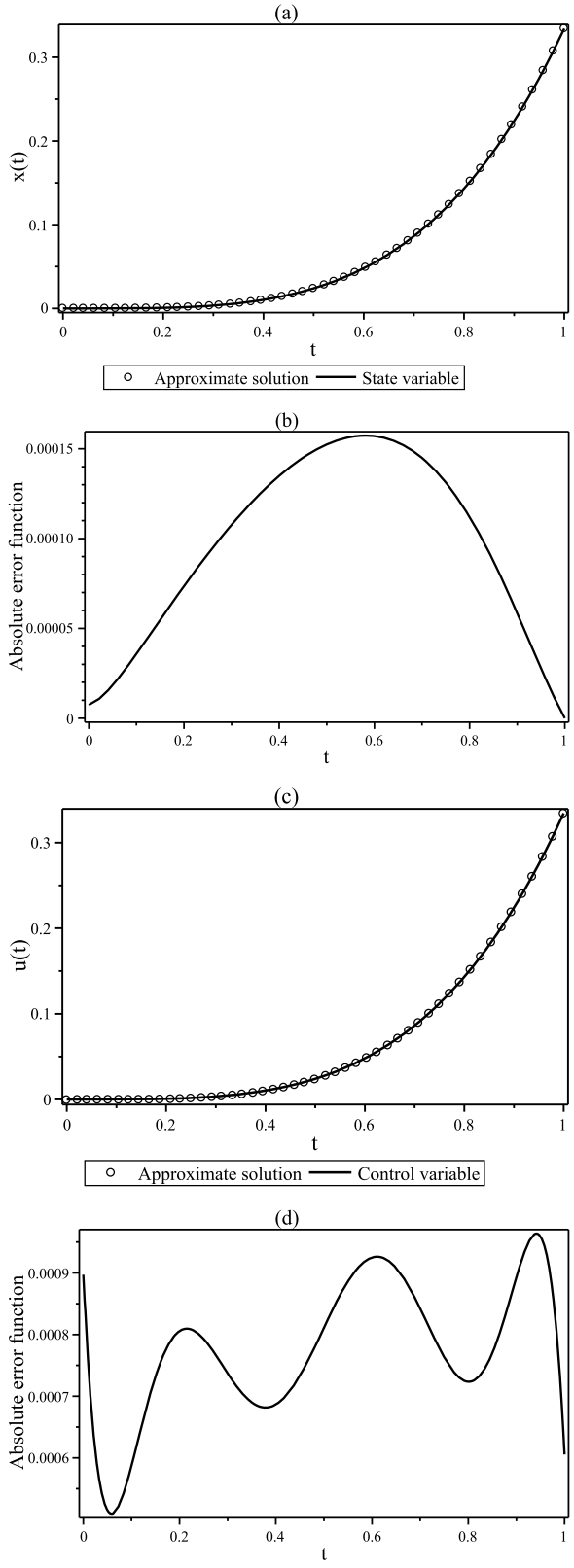

Figure 3: Plots of (a) approximate solutions for $\mathrm{x}(t)$, (b) approximate solutions for $\mathrm{u}(t)$, (c) absolute error function of $\mathrm{x}(t)$, (d) absolute error function of $\mathrm{u}(t)$ for $N = 7$ and $\theta(t) = 0.8 + 0.005\sin(t)$ of Example 6.2.

Example 6.2. Consider the following VOCP [42]

$$\mathrm{Min}\,\mathcal{J}[\mathrm{x},\mathrm{u}] = \int_0^1 (\mathrm{u}(t) - \mathrm{x}(t))^2 \mathrm{d}t,$$

$$\dot{\mathrm{x}}(t) + {}_0^C\mathcal{D}_t^{\theta(t)}\mathrm{x}(t) - \mathrm{u}(t) + \mathrm{x}(t) - t^3 - \frac{6t^{\theta(t)+2}}{\Gamma(\theta(t)+3)} = 0, \quad 0 < \theta(t) \leqslant 1,$$

with

$$\mathrm{x}(0) = 0, \quad \mathrm{x}(1) = \frac{6}{\Gamma(\theta(1)+4)}.$$

The exact solutions are $(\mathrm{x}(t), \mathrm{u}(t), \mathcal{J}[\mathrm{x},\mathrm{u}]) = \left(\frac{6t^{\theta(t)+3}}{\Gamma(\theta(t)+4)}, \frac{6t^{\theta(t)+3}}{\Gamma(\theta(t)+4)}, 0\right)$. The values of the absolute errors of $\mathrm{x}(t)$ and $\mathrm{u}(t)$ at the equally spaced points $t_i = 0.1i$, $i = 0, 1, \ldots, 10$, are listed in Table 3 for $N = 5$ and $\theta(t) = 0.45, 0.47, 0.49$. The optimal values of the functional $\mathcal{J}[\mathrm{x},\mathrm{u}]$ are listed in Table 4 for $N = 5$ and $\theta(t) = 0.7, 0.8, 0.9, 1$, and compared to the values reported in [19] and [42]. It can be seen that the accuracy of the approximate solutions increases when $\theta(t) \to 1$. The computational time for this algorithm is 1.17 s. By choosing functions $\theta_i(t)$, $i = 1, 2, 3, 4$, as

$$\theta_1(t) = 0.8 + 0.05\sin(t), \quad \theta_2(t) = 0.8 + 0.005\sin(t), \quad \theta_3(t) = 0.8 + 0.0005\sin(t), \quad \theta_4(t) = 0.8,$$

the values of the performance index are listed in Table 5 for $N = 7$ and the values are compared to results in [19]. Values of absolute errors at equally spaced points $t_i = 0.2i$, $i = 0, 1, \ldots, 5$ are listed in Table 6. The running

Table 7: Absolute errors of optimal approximate solutions for $N = 10$ and $\theta(t) = 1$ of Example 6.3

	Present method		Method in [48]		Method in [19]	
t_i	$\mathrm{x}_N(t)$	$\mathrm{u}_N(t)$	$\mathrm{x}_N(t)$	$\mathrm{u}_N(t)$	$\mathrm{x}_N(t)$	$\mathrm{u}_N(t)$
0	0	3.0459×10^{-4}	—	—	8.29×10^{-17}	8.61×10^{-6}
0.2	1.3391×10^{-6}	7.2656×10^{-5}	5.60×10^{-5}	2.92×10^{-5}	1.48×10^{-7}	1.39×10^{-6}
0.4	3.0578×10^{-6}	4.0056×10^{-5}	2.75×10^{-5}	5.10×10^{-6}	1.85×10^{-7}	6.00×10^{-7}
0.6	2.9100×10^{-6}	3.6618×10^{-5}	1.16×10^{-5}	1.87×10^{-5}	1.86×10^{-7}	6.93×10^{-7}
0.8	1.3890×10^{-6}	7.1999×10^{-5}	4.65×10^{-6}	3.96×10^{-5}	1.47×10^{-7}	1.37×10^{-6}
1	7.8391×10^{-9}	2.9045×10^{-5}	1.62×10^{-6}	2.27×10^{-3}	2.71×10^{-12}	7.65×10^{-6}
$\mathcal{J}[\mathrm{x},\mathrm{u}]$	0.19290929598		—		0.19290929809	

Table 8: Maximum absolute errors of $\mathrm{x}(t)$ and $\mathrm{u}(t)$ and estimated values of $\mathcal{J}[\mathrm{x},\mathrm{u}]$ for $N = 8$, and various values of $\theta(t)$ of Example 6.3

Present method	$\theta(t) = 1 - 0.05t$	$\theta(t) = 1 - 0.03t$	$\theta(t) = 1 - 0.01t$
Error of $\mathrm{x}(t)$	4.6499×10^{-3}	2.8138×10^{-3}	9.9235×10^{-4}
Error of $\mathrm{u}(t)$	5.7571×10^{-3}	3.5361×10^{-3}	1.8784×10^{-3}
$\mathcal{J}[\mathrm{x},\mathrm{u}]$	0.19395417611	0.19353733279	0.19311893574
Method in [19]	$\theta(t) = 1 - 0.05t$	$\theta(t) = 1 - 0.03t$	$\theta(t) = 1 - 0.01t$
Error of $\mathrm{x}(t)$	1.13×10^{-2}	6.80×10^{-3}	2.27×10^{-3}
Error of $\mathrm{u}(t)$	6.30×10^{-3}	3.71×10^{-3}	1.21×10^{-3}
$\mathcal{J}[\mathrm{x},\mathrm{u}]$	0.1933774618	0.19319043961	0.19300305529

time is 4.71 s. The plots of the error functions of $\mathrm{x}(t)$ and $\mathrm{u}(t)$ are depicted in Figure 2 for $N = 5$ and $\theta(t) = 0.7$. The figures of the approximate optimal solutions are shown in Figure 3 for $\theta(t) = 0.8 + 0.005\sin(t)$ and $N = 7$.

Example 6.3. The following VOCP is considered [19,48]:

$$\mathrm{Min}\,\mathcal{J}[\mathrm{x},\mathrm{u}] = \frac{1}{2}\int_0^1 (\mathrm{x}^2(t) + \mathrm{u}^2(t))\mathrm{d}t,$$
$$ {}_0^C\mathcal{D}_t^{\theta(t)}\mathrm{x}(t) + \mathrm{x}(t) - \mathrm{u}(t) = 0, \quad 0 < \theta(t) \leqslant 1,$$

with the initial condition

$$\mathrm{x}(0) = 1.$$

If $\theta(t) = 1$, the exact solutions are

$$\mathrm{x}(t) = \cosh(\sqrt{2}\,t) + \beta\sinh(\sqrt{2}\,t), \quad \mathrm{u}(t) = (1 + \sqrt{2}\beta)\cosh(\sqrt{2}\,t) + (\sqrt{2} + \beta)\sinh(\sqrt{2}\,t),$$

where

$$\beta = -\frac{\cosh(\sqrt{2}) + \sqrt{2}\sinh(\sqrt{2})}{\sqrt{2}\cosh(\sqrt{2}) + \sinh(\sqrt{2})},$$

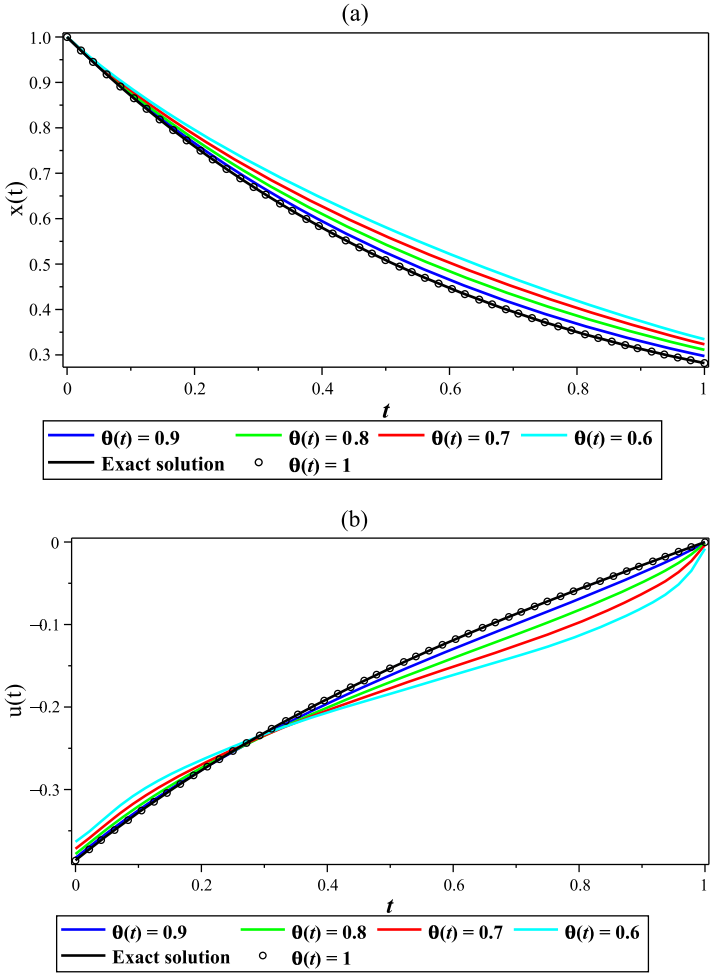

Figure 4: Plots of approximate solutions of (a) $\mathrm{x}(t)$, (b) $\mathrm{u}(t)$ for $N = 10$, and various values of $\theta(t)$ of Example 6.3.

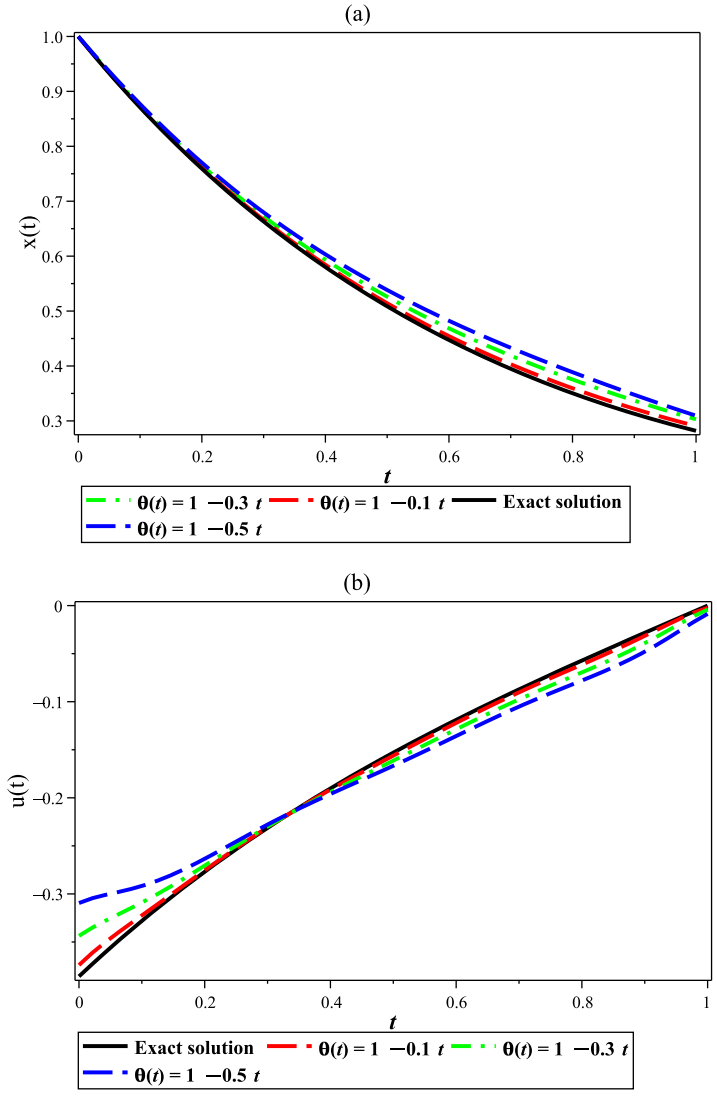

Figure 5: Plots of approximate solutions of (a) $\mathrm{x}(t)$, (b) $\mathrm{u}(t)$ for $N = 8$, and various values of $\theta(t)$ of Example 6.3.

Table 9: Estimated values of $\mathcal{J}[\mathrm{x}, \mathrm{u}]$ for $N = 6$, and various values of $\theta(t)$ of Example 6.4

	$\boldsymbol{\theta(t) = 0.75 + 0.2\sin(50t)}$	$\boldsymbol{\theta(t) = 0.75 + 0.2\sin(30t)}$	$\boldsymbol{\theta(t) = 0.75 + 0.2\sin(10t)}$	$\boldsymbol{\theta(t) = 1}$
Present method	1.1661×10^{-2}	9.1085×10^{-3}	7.1967×10^{-3}	1.2905×10^{-13}
Method in [19]	3.7253×10^{-3}	1.2466×10^{-3}	5.7619×10^{-3}	4.2655×10^{-9}

Table 10: Estimated values of $\mathcal{J}[\mathrm{x}, \mathrm{u}]$ for $N = 6$ and different values of $\theta(t)$ of Example 6.4

	$\boldsymbol{\theta(t) = 0.85}$	$\boldsymbol{\theta(t) = 0.9}$	$\boldsymbol{\theta(t) = 0.95}$	$\boldsymbol{\theta(t) = 1}$
$\mathcal{J}[\mathrm{x}, \mathrm{u}]$	1.4602×10^{-3}	6.6526×10^{-4}	1.7033×10^{-4}	1.2905×10^{-13}

Table 11: Errors of optimal approximate solutions at selected points and estimated values of $\mathcal{J}[x, u]$ for $N = 4, 6$ and $\theta(t) = 1$ of Example 6.4

	$N = 4$		$N = 6$	
t_i	$x_N(t)$	$u_N(t)$	$x_N(t)$	$u_N(t)$
0	0	1.9608×10^{-4}	0	1.6891×10^{-6}
0.2	7.0998×10^{-7}	1.4569×10^{-5}	4.6029×10^{-8}	3.4978×10^{-7}
0.4	4.0818×10^{-6}	3.5354×10^{-5}	6.9652×10^{-8}	1.9184×10^{-7}
0.6	1.4641×10^{-5}	2.8243×10^{-5}	1.0007×10^{-7}	3.2709×10^{-8}
0.8	3.2017×10^{-6}	2.5048×10^{-5}	3.7045×10^{-8}	2.1652×10^{-7}
1	3.9543×10^{-6}	4.7536×10^{-7}	7.0014×10^{-8}	1.2514×10^{-6}
$\mathcal{J}[x, u]$	1.4754×10^{-9}		1.2905×10^{-13}	

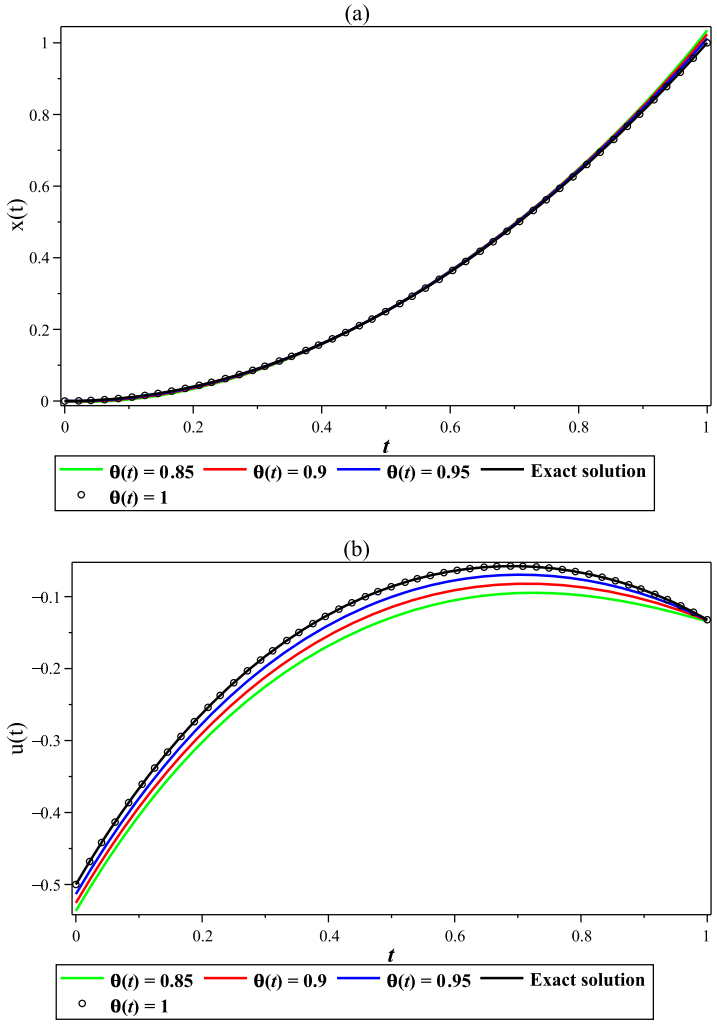

Figure 6: Plots of approximate solutions of (a) $x(t)$, (b) $u(t)$ for $N = 6$, and various values of $\theta(t)$ of Example 6.4.

and $\mathcal{J}[x, u] = 0.1929092980931693$. The values of the absolute errors of the approximate solutions are listed in Table 7 at the points $t_i = 0.2i$, $i = 0, 1, \ldots, 5$, $N = 10$, and $\theta(t) = 1$ and compared to results in [19] and [48]. The maximum absolute errors of $x(t)$ and $u(t)$ and the approximate values of $\mathcal{J}[x, u]$ are observed in Table 8 for

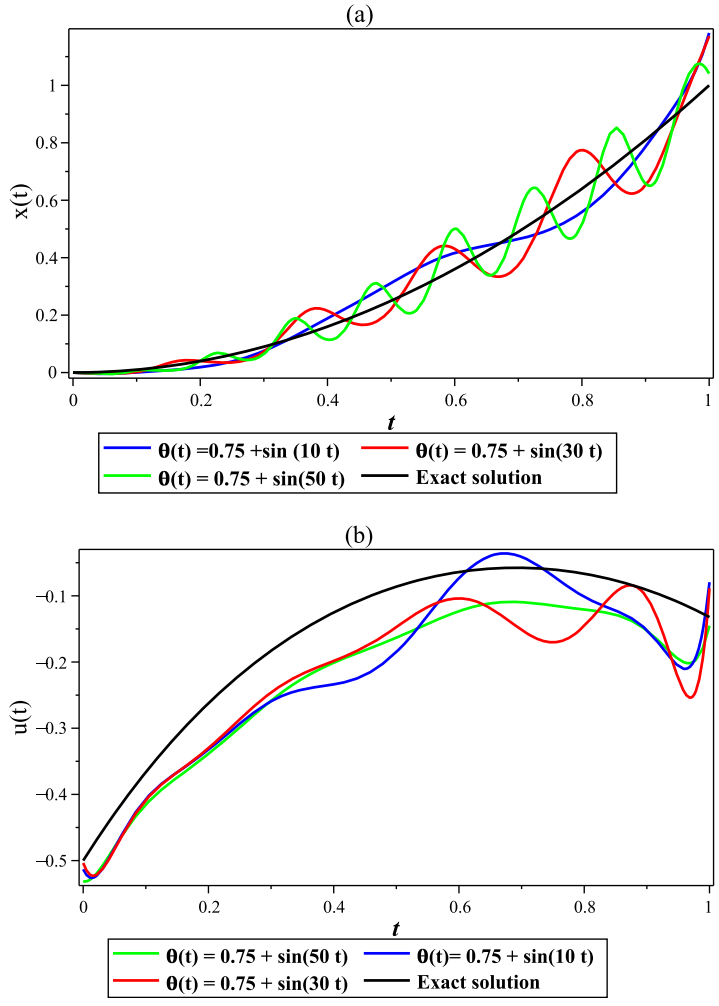

Figure 7: Plots of approximate solutions of (a) $\mathrm{x}(t)$, (b) $\mathrm{u}(t)$ for $N = 10$, and various values of $\theta(t)$ of Example 6.4.

Table 12: Convergence rate of obtained solutions for $\theta(t) = 1$ and various values of N for Example 6.4

N	$\mathrm{x}_N(t)$	CR_{x}	$\mathrm{u}_N(t)$	CR_{u}
2	9.5990×10^{-4}		1.7353×10^{-2}	
3	8.3673×10^{-4}		5.9933×10^{-3}	
4	1.4743×10^{-5}	6.0248	1.9609×10^{-4}	6.4675
5	1.2929×10^{-5}		8.5517×10^{-5}	
6	1.0014×10^{-7}	12.4675	1.6891×10^{-6}	11.7257
7	1.2140×10^{-8}		1.8502×10^{-7}	
8	1.2027×10^{-9}	15.3711	2.1180×10^{-8}	15.2213

various values of $\theta(t)$ and $N = 10$ and the results are compared to results in [19]. The plots of the approximate solutions are seen in Figure 4 for $N = 10$ and $\theta(t) = 0.6, 0.7, 0.8, 0.9, 1$. The plots of approximate solutions for $N = 8$ and $\theta_1(t) = 1 - 0.1t$, $\theta_2(t) = 1 - 0.3t$, and $\theta_3(t) = 1 - 0.5t$ are shown in Figure 5.

Example 6.4. Consider the following VOCP [19,24]:

$$\mathrm{Min}\,\mathcal{J}[\mathrm{x},\mathrm{u}] = \int_0^1 \left((\mathrm{x}(t) - t^2)^2 + (\mathrm{u}(t) - te^{-t} + \frac{1}{2}e^{t^2-t})^2\right)\mathrm{d}t,$$
$${}_0^C\mathcal{D}_t^{\theta(t)}\mathrm{x}(t) - e^{\mathrm{x}(t)} - 2e^t\mathrm{u}(t) = 0, \quad 0 < \theta(t) \leqslant 1,$$

with the initial condition

$$\mathrm{x}(0) = 0.$$

If $\theta(t) = 1$, then the exact solutions are $(\mathrm{x}(t), \mathrm{u}(t), \mathcal{J}[\mathrm{x},\mathrm{u}]) = (t^2, te^{-t} - \frac{1}{2}e^{t^2-t}, 0)$. The approximate values of $\mathcal{J}[\mathrm{x},\mathrm{u}]$ are listed in Table 9 for $N = 6$ and different values of $\theta(t)$ and compared to the results reported in [19]. Also, the obtained approximate values of functional $\mathcal{J}[\mathrm{x},\mathrm{u}]$ are listed in Table 10 for $N = 6$ and $\theta(t) = 0.85, 0.9, 0.95, 1$. The approximate values of $\mathrm{x}(t)$ and $\mathrm{u}(t)$ at the points t_i, $0 \leqslant i \leqslant 5$, and the estimated values of $\mathcal{J}[\mathrm{x},\mathrm{u}]$ are computed and observed in Table 11 for $N = 4, 6$ and $\theta = 1$. As shown, by increasing the value of N, the accuracy of the scheme increases as well. The figures of the approximate solutions are plotted in Figure 6 for $N = 6$ and $\theta(t) = 0.85, 0.9, 0.95, 1$. Figure 7 displays exact and approximate solutions for $N = 10$ and $\theta(t) = 0.75 + 0.2\sin(10t)$, $\theta(t) = 0.75 + 0.2\sin(30t)$, $\theta(t) = 0.75 + 0.2\sin(50t)$. The convergence rate is computed by the following formula:

$$CR_z = \frac{|\ln(E_{2i}/E_{2i-2})|}{|\ln(2i/2i-2)|},$$

where E_j is computed by the absolute error calculated for series solution including $j + 1$ basis functions and $z = \mathrm{x}(t)$ or $\mathrm{u}(t)$. Convergence rates of obtained solutions are listed in Table 12 for $\theta(t) = 1$ and diverse values of N.

7 Conclusion

The present paper introduced an operational collocation approach established upon the SCPs to deal with a category of optimal control problems involving a VODS. As a result, the objective function is replaced by an algebraic equation, and the VODS is replaced by a system of algebraic equations. By using the Lagrange multipliers method, the constrained equations derived from joining the objective function to the VODS are optimized. Using a Chebyshev-weighted Sobolev space, convergence bounds showed that the method error will be small enough when N is large enough. The obtained results were compared to the exact solutions and the results reported by the other authors. Tables and figures clearly demonstrate that the proposed method can be utilized as a reliable and efficient tool for solving variable-order functional equations.

Acknowledgement: Authors are very grateful to anonymous referees for their careful reading and valuable comments which led to the improvement of this study.

Funding information: Not applicable.

Author contributions: Data curation, formal analysis, investigation, methodology, software, and writing – original draft: Khadijeh Sadri; data curation, resources, validation, and writing – review and editing: Kamyar Hosseini; resources, supervision, visualization, and writing – review and editing: Soheil Salahshour, Dumitru Baleanu, Ali Ahmadian, and Choonkil Park; and funding acquisition: Choonkil Park. Authors declare that the study was carried out collaboratively with a division of responsibilities. All authors read and approved the final manuscript.

Conflict of interest: The authors declare that they have no known competing financial interests or personal relationships that could have appeared to influence the work reported in this article.

Ethical approval: The conducted research is not related to either human or animal use.

Data availability statement: Data sharing is not applicable to this article as no datasets were generated or analyzed during the current study.

References

[1] L. Beghin and M. Caputo, *Commutative properties of the Caputo fractional derivative and its generalizing convolution operator*, Commun. Nonlinear Sci. Numer. Simul. **89** (2020), 105338, DOI: https://doi.org/10.1016/j.cnsns.2020.105338.

[2] T. Blaszczyk, K. Bekus, K. Szajek, and W. Sumelko, *On numerical approximation of the Riesz-Caputo operator with the fixed/short memory length*, J. King Saud Univ. Sci. **33** (2021), no. 1, 101220, DOI: https://doi.org/10.1016/j.jksus.2020.10.017.

[3] M. C. Neel, A. Abdennadher, and J. Solofoniaina, *A continuous variant for Grunwald-Letnikov fractional derivatives*, Phys. A **387** (2008), no. 12, 2750–2760, DOI: https://doi.org/10.1016/j.physa.2008.01.090.

[4] A. Haq and N. Sukavanam, *Existence and approximate controllability of Riemann-Liouville fractional integro-differential systems with damping*, Chaos Solitons Fractals **139** (2020), 110043, DOI: https://doi.org/10.1016/j.chaos.2020.110043.

[5] G. Wang, K. Pei, R. P. Agarwal, L. Zhang, and B. Ahmad, *Nonlocal Hadamard fractional boundary value problem with Hadamard integral and discrete boundary conditions on a half-line*, J. Comput. Appl. Math. **343** (2018), 230–239, DOI: https://doi.org/10.1016/j.cam.2018.04.062.

[6] K. Tao, H. Chen, W. L. Peng, J. Yao, and Y. Wu, *A new method on Box dimension of Weyl-Marchaud fractional derivative of Weierstrass function*, Chaos Soliton Fractals **142** (2021), 110317, DOI: https://doi.org/10.1016/j.chaos.2020.110317.

[7] X. Zheng, H. Wang, and H. Fu, *Analysis of a physically-relevant variable-order time-fractional reaction-diffusion model with Mittag-Leffler kernel*, Appl. Math. Lett. **112** (2021), 106804, DOI: https://doi.org/10.1016/j.aml.2020.106804.

[8] H. Tajadodi, *Efficient technique for solving variable order fractional optimal control problems*, Alex. Eng. J. **59** (2020), no. 6, DOI: https://doi.org/10.1016/j.aej.2020.09.047.

[9] L. Wei and Y. Yang, *Optimal order finite difference/local discontinuous Galerkin method for variable-order time-fractional diffusion equation*, J. Comput. Appl. Math. **383** (2021), 113129, DOI: https://doi.org/10.1016/j.cam.2020.113129.

[10] Z. Yang, X. Zheng, Z. Zheng, and H. Wang, *Strong convergence of an Euler-Maruyama scheme to a variable-order fractional stochastic differential equation driven by a multiplicative white noise*, Chaos Solitons Fractals **142** (2021), 110392, DOI: https://doi.org/10.1016/j.chaos.2020.110392.

[11] N. H. Sweilam, S. M. Al-Mekhlafi, Z. N. Mohammed, and D. Baleanu, *Optimal control for variable order fractional HIV/AIDS and Malaria mathematical models with multi-time delay*, Alex. Eng. J. **59** (2020), no. 5, 3149–3162, DOI: https://doi.org/10.1016/j.aej.2020.07.021.

[12] F. Wu, R. Gao, and C. Li, *New fractional variable-order creep model with short memory*, Appl. Math. Comput. **380** (2020), 125278, DOI: https://doi.org/10.1016/j.amc.2020.125278.

[13] N. Sweilam, S. Al-Mekhlafi, S. Shatta, and D. Baleanu, *Numerical study for two type variable-order Burgers' equations with proportional delay*, Appl. Numer. Math. **156** (2020), 364–376, DOI: https://doi.org/10.1016/j.apnum.2020.05.006.

[14] H. Dehestani, Y. Ordokhani, and M. Razzaghi, *Application of fractional of Gegenbauer functions in variable-order fractional delay-type equations with non-singular kernel derivatives*, Chaos Solitons Fractals **140** (2020), 110111, DOI: https://doi.org/10.1016/j.chaos.2020.110111.

[15] X. Li and B. Wu, *Reproducing kernel functions-based meshless method for variable order fractional advection-diffusion-reaction equations*, Alex. Eng. J. **59** (2020), no. 5, 3181–3186, DOI: https://doi.org/10.1016/j.aej.2020.07.034.

[16] M. Kashif, P. Pandey, and H. Jafari, *A novel numerical manner for non-linear coupled variable order reaction-diffusion equation*, Therm. Sci. **27** (2023), no. 1, 353–363, DOI: https://doi.org/10.2298/TSCI23S1353K.

[17] R. M. Ganji and H. Jafari, *A numerical approach for multi-variable orders differential equations using Jacobi polynomials*, Int. J. Appl. Comput. Math. **5** (2019), 34, DOI: https://doi.org/10.1007/s40819-019-0610-6.

[18] H. Jafari, S. Nemati, and R. M. Ganji, *Operational matrices based on the shifted fifth-kind Chebyshev polynomials for solving nonlinear variable order integro-differential equations*, Adv. Differential Equations **2021** (2021), 435, DOI: https://doi.org/10.1186/s13662-021-03588-2.

[19] H. Dehestani, Y. Ordokhani, and M. Razzaghi, *Fractional-order Bessel wavelet functions for solving variable order fractional optimal control problems with estimation error*, Internat. J. Systems Sci. **56** (2020), no. 6, 1032–1052, DOI: https://doi.org/10.1080/00207721.2020.1746980.

[20] M. H. Heydari, M. R. Mahmoudi, Z. Avazzadeh, and D. Baleanu, *Chebyshev cardinal functions for a new class of nonlinear optimal control problems with dynamical systems of weakly singular variable-order fractional integral equations*, J. Vib. Control **26** (2020), no. 9–10, DOI: https://doi.org/10.1177/1077546319889862.

[21] O. P. Agrawal, *A general formulation and solution scheme for fractional optimal control problem*, Nonlinear Dyn. **38** (2004), 323–337, DOI: https://doi.org/10.1007/s11071-004-3764-6.
[22] H. Hassani and Z. Avazzadeh, *Transcendental Bernstein series for solving non-linear variable-order fractional optimal control problems*, Appl. Math. Comput. **362** (2019), 124563, DOI: https://doi.org/10.1016/j.amc.2019.124563.
[23] M. H. Heydari, *A new direct method based on the Chebyshev cardinal functions for variable-order fractional optimal control problems*, J. Franklin Inst. **355** (2018), no. 12, 4970–4995, DOI: https://doi.org/10.1016/j.jfranklin.2018.05.025.
[24] M. H. Heydari and Z. Avazzadeh, *A new wavelet method for variable-order fractional optimal control problems*, Asian J. Control **20** (2018), no. 5, 1804–1817, DOI: https://doi.org/10.1002/asjc.1687.
[25] M. A. Zaky and A Legendre *collocation method for distributed-order fractional optimal control problems*, Nonlinear Dyn. **91** (2018), 2667–2681, DOI: https://doi.org/10.1007/s11071-017-4038-4.
[26] M. A. Zaky, *A research note on the nonstandard finite difference method for solving variable-order fractional optimal control problems*, J. Vib. Control **24** (2018), no. 11, 2109–2111, DOI: https://doi.org/10.1177/1077546318761443.
[27] M. R. A. Sarkan, *Numerical solutions of integral and integro-differential equations using Chebyshev polynomials of the third kind*, Appl. Math. Comput. **351** (2019), 66–82, DOI: https://doi.org/10.1016/j.amc.2019.01.030.
[28] D. S. Mohamed and R. A. Taher, *Comparison of Chebyshev and Legendre polynomials methods for solving two dimensional Volterra-Fredholm integral equations*, J. Egyptian Math. Soc. **25** (2017), no. 3, 302–307, DOI: https://doi.org/10.1016/j.joems.2017.03.002.
[29] H. Singh and C. S. Singh, *A reliable method based on second kind Chebyshev polynomial for the fractional model of Bloch equation*, Alex. Eng. J. **57** (2018), no. 3, 1425–1432, DOI: https://doi.org/10.1016/j.aej.2017.07.002.
[30] N. H. Sweilam, A. M. Nagy, and A. A. El-Sayed, *Second kind shifted Chebyshev polynomials for solving space fractional order diffusion equation*, Chaos Solitons Fractals **73** (2015), 141–147, DOI: https://doi.org/10.1016/j.chaos.2015.01.010.
[31] N. H. Sweilam, A. M. Nagy, and A. A. El-sayed, *On the numerical solution of space fractional order diffusion equation via shifted Chebyshev polynomials of the third kind*, J. King Saud Univ. Sci. **28** (2016), no. 1, 41–47, DOI: https://doi.org/10.1016/j.jksus.2015.05.002.
[32] M. Gulsu, Y. Ozturk, and M. Sezer, *On the solution of the Abel equation of the second kind by the shifted Chebyshev polynomials*, Appl. Math. Comput. **217** (2011), no. 9, 4827–4833, DOI: https://doi.org/10.1016/j.amc.2010.11.044.
[33] B. K. Gimire, X. Li, C. S. Chen, and A. R. Lami Chhane, *Hybrid Chebyshev polynomials scheme for solving elliptic partial differential equations*, J. Comput. Appl. Math. **364** (2020), 112324, DOI: https://doi.org/10.1016/j.cam.2019.06.040.
[34] W. M. Abd-Elhameed and Y. H. Youssri, *Fifth-kind orthonormal Chebyshev polynomial solutions for fractional differential equations*, Comput. Appl. Math. **37** (2018), 2897–2921, DOI: https://doi.org/10.1007/s40314-017-0488-z.
[35] R. M. Ganji, H. Jafari, and D. Baleanu, *A new approach for solving multi variable orders differential equations with Mittag-Leffler kernel*, Chaos Solitons Fractals **130** (2020), 109405, DOI: https://doi.org/10.1016/j.chaos.2019.109405.
[36] W. M., Abd-Elhameed and Y. H. Youssri, *Sixth-kind Chebyshev spectral approach for solving fractional differential equations*, Int. J. Nonlinear Sci. Numer. Simul. **20** (2019), no. 2, 191–203, DOI: https://doi.org/10.1515/ijnsns-2018-0118.
[37] M. Masjed-Jamei, *Some new classes of orthogonal polynomials and special functions: A symmetric generalization of Sturm-Liouville problems and its consequences*, Department of Mathematics, University of Kassel, 2006.
[38] H. Jafari, A. Babaei, S. Banihashemi, and A Novel *Approach for Solving an Inverse Reaction-Diffusion-Convection Problem*, J. Optim. Theory Appl. **183** (2019), 688–704, DOI: https://doi.org/10.1007/s10957-019-01576-x.
[39] A. Babaei, H. Jafari, and S. Banihashemi, *Numerical solution of variable order fractional nonlinear quadratic integro-differential equations based on the sixth-kind Chebyshev collocation method*, J. Comput. Appl. Math. **377** (2020), 112908, DOI: https://doi.org/10.1016/j.cam.2020.112908.
[40] A. G. Atta, W. M. Abd-Elhameed, G. M. Moatimid, and Y. H. Youssri *A fast Galerkin approach for solving the fractional Rayleigh-Stokes problem via sixth-kind Chebyshev polynomials*, Mathematics **20** (2022), no. 11, 1843, DOI: https://doi.org/10.3390/math10111843.
[41] A. G. Atta, W. M. Abd-Elhameed, G. M. Moatimid, and Y. H. Youssri, *Advanced shifted sixth-kind Chebyshev Tau approach for solving linear one-dimensional hyperbolic telegraph type problem*, Math. Sci. **17** (2023), 415–429.
[42] K. Rabiei, Y. Ordokhani, and E. Babolian, *Numerical solution of 1D and 2D fractional optimal control of system via Bernoulli polynomials*, Int. J. Appl. Comput. Math. **4** (2018), DOI: https://doi.org/10.1007/s40819-017-0435-0.
[43] K. Sadri and H. Aminikhah, *An efficient numerical method for solving a class of fractional mobile-immobile advection-dispersion equations and its convergence analysis*, Chaos Solitons Fractals **146** (2021), 110896, DOI: https://doi.org/10.1016/j.chaos.2021.110896.
[44] A. Borhanifar and Kh. Sadri, *A new operational approach for numerical solution of generalized functional integro-differential equations*, J. Comput. Appl. Math. **279** (2015), 80–96, DOI: https://doi.org/10.1016/j.cam.2014.09.031.
[45] G. W. Stewart, *Matrix Algorithms*, SIAM, Philadelphia, 1998.
[46] C. Canuto, M. Y. Hussaini, A. Quarteroni, and T. A. K. Zang, *Spectral methods: Fundamentals in Single Domains*, Springer, Berlin, Heidelberg, 2006, DOI: https://doi.org/10.1007/978-3-540-30726-6.
[47] N. H. Sweilam and T. M. Al-Ajami, *Legendre spectral-collocation method for solving some types of fractional optimal control problems*, J. Adv. Res. **6** (2015), no. 3, 393–403, DOI: https://doi.org/10.1016/j.jare.2014.05.004.
[48] M. H. Heydari, M. R. Hooshmandasl, F. M. Maalek Ghaini, and C. Cattani, *Wavelets method for solving fractional optimal control problems*, Appl. Math. Comput. **286** (2016), 139–154, DOI: https://doi.org/10.1016/j.amc.2016.04.009.

Appendix

An upper bound can be presented to estimate the error of the operational matrix in Theorem 3.2.

Consider the following error vector:

$$\mathcal{E}(t) = \int_0^t \mathbf{Y}(s)\mathrm{d}s - \mathbf{P}\mathbf{Y}(t) = [E_0(t), E_1(t), \ldots, E_N(t)]^T,$$

where

$$E_j(t) = \int_0^t \mathcal{Y}_j(s)\mathrm{d}s - \mathbf{P}_j\mathbf{Y}(t), \quad j = 0, 1, \ldots, N,$$

and $\mathbf{P}_j$ is the jth row of the operational matrix $\mathbf{P}$. Let $g_j(t) = \int_0^t \mathcal{Y}_j(s)\mathrm{d}s$. According to the definition of the semi-norm in the space $\mathcal{CH}_w^{\varpi}(J)$, one obtains

$$\begin{aligned}
|g_j(t)|^2_{\mathcal{CH}_w^{\varpi,N}(J)} &= \sum_{k=\min\{\varpi,N+1\}}^{\varpi} \left\| \frac{\mathrm{d}^k}{\mathrm{d}t^k} \int_0^t \mathcal{Y}_j(s)\mathrm{d}s \right\|^2_{L^2_w(J)} \\
&= \sum_{k=\min\{\varpi,N+1\}}^{\varpi} \left\| \sum_{r=k-1}^{j} \varsigma_{r,j} \frac{\Gamma(r+1)t^{r-k+1}}{\Gamma(r-k+2)} \right\|^2_{L^2_w(J)} \\
&= \sum_{k=\min\{\varpi,N+1\}}^{\varpi} \sum_{r=k-1}^{j} \sum_{s=k-1}^{j} \varsigma_{r,j}\varsigma_{s,j} \frac{\Gamma(r+1)\Gamma(s+1)}{\Gamma(r-k+2)\Gamma(s-k+2)} \\
&\quad \times \int_0^1 \left(4t^{r+s-2k+\frac{9}{2}} - 4t^{r+s-2k+\frac{7}{2}} + t^{r+s-2k+\frac{5}{2}}\right)(1-t)^{\frac{1}{2}}\mathrm{d}t \\
&= \sum_{k=\min\{\varpi,N+1\}}^{\varpi} \sum_{r=k-1}^{j} \sum_{s=k-1}^{j} \varsigma_{r,j}\varsigma_{s,j} \frac{\Gamma(r+1)\Gamma(s+1)\Gamma(\frac{3}{2})}{\Gamma(r-k+2)\Gamma(s-k+2)} \left(4\frac{\Gamma(r+s-2k+\frac{11}{2})}{\Gamma(r+s-2k+7)} - 4\frac{\Gamma(r+s-2k+\frac{9}{2})}{\Gamma(r+s-2k+6)} \right. \\
&\quad \left. + \frac{\Gamma\left(r+s-2k+\frac{7}{2}\right)}{\Gamma(r+s-2k+5)} \right) = \mathcal{Z}_j^{\varpi 2}, \quad j = 0, 1, \ldots, N.
\end{aligned}$$

Now, by utilizing Theorem 5.1, one yields the following error bound:

$$\|E_j\|_{L^2_w(J)} \leq \beta N^{-\varpi} \mathcal{Z}_j, \quad j = 0, 1, \ldots, N.$$

Similarly, a bound for the error of this approximation can be obtained.